

The logo for Temple Materials Institute (TMI) features the letters 'TMI' in a bold, blue, serif font on a yellow background.The logo for Temple Materials Institute (TMI) features the text 'TEMPLE MATERIALS INSTITUTE' in a blue, sans-serif font on a yellow background.

College of
Science and Technology
TEMPLE UNIVERSITY®

**What can SCAN do for Molecules and
Materials ..? Liquids, Crystals, Liquid
Crystals, Plastic Crystals, & More ...**

**Michael L. Klein, FRS
Temple University
Philadelphia PA 19122 USA**

The logo for the Institute for Computational Molecular Science (ICMS) features a stylized blue graphic of overlapping spheres and a blue ribbon on the left, followed by the letters 'ICMS' in a large, white, serif font.

Institute for Computational Molecular Science



The logo for Temple Materials Institute (TMI) features the letters 'TMI' in a bold, blue, serif font on a yellow rectangular background.The logo for Temple Materials Institute (TMI) features the text 'TEMPLE MATERIALS INSTITUTE' in a blue, sans-serif font on a yellow arrow-shaped background pointing to the right.

College of
Science and Technology
TEMPLE UNIVERSITY®

**The understanding of Liquid & Solid Phases is inextricably linked both to theory & computer simulation ..
The latter brings insights and unique contributions to help rationalize the diversity exhibited by Nature ...**

The logo for the Institute for Computational Molecular Science (ICMS) features a blue background with a stylized, glowing blue molecular structure on the left and the letters 'ICMS' in a large, white, serif font on the right. Below the main text, the full name 'Institute for Computational Molecular Science' is written in a smaller, white, sans-serif font.

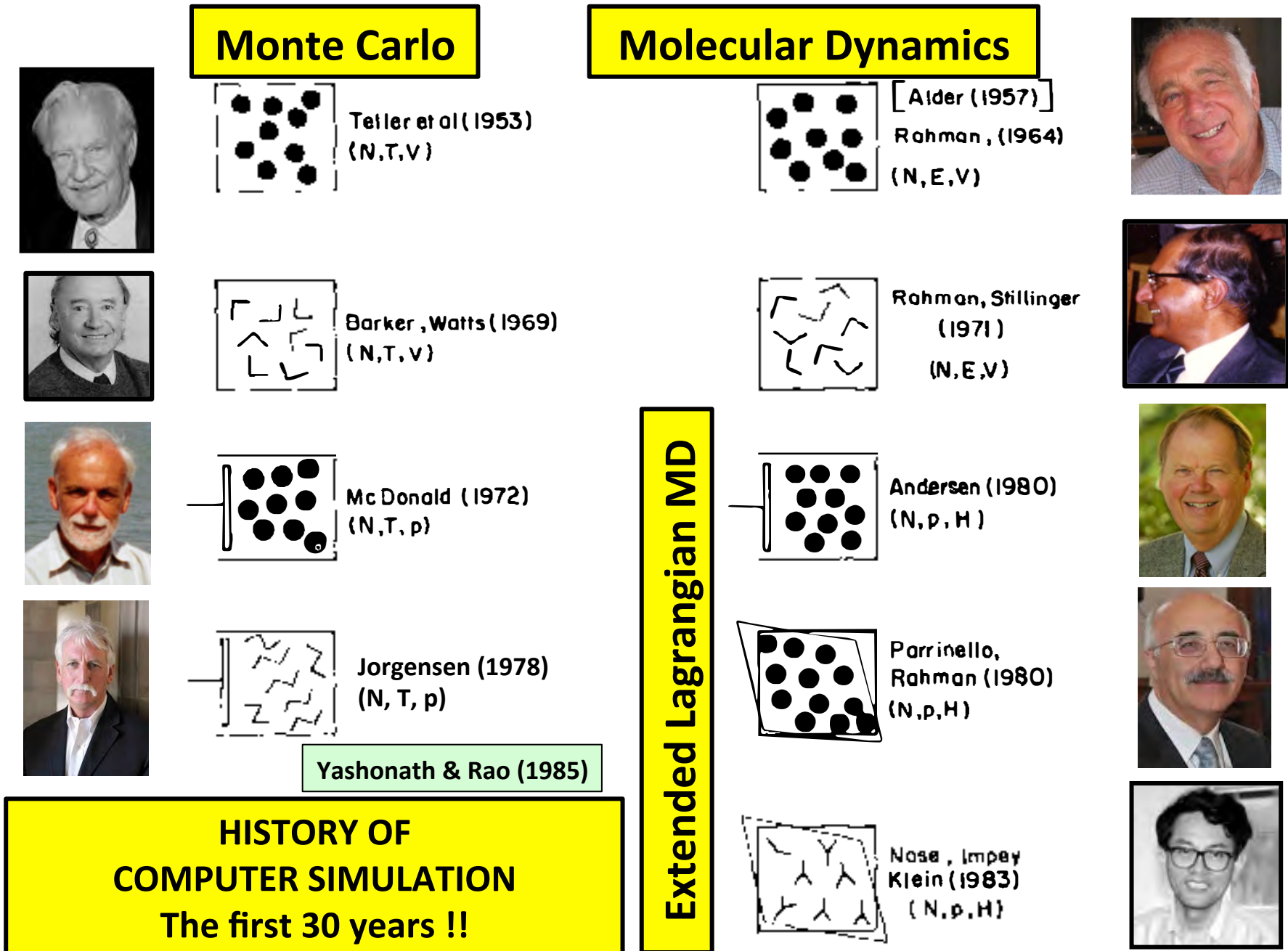


Figure 3 The genealogy of black boxes available for simulation work (see text).

Resource for first part of the talk

COMPUTER SIMULATION STUDIES OF SOLIDS

Michael L. Klein

**Extended Lagrangian Dynamics:
Andersen, Parrinello & Rahman:**
The “new” MD, before CP-MD ..

$$\mathcal{L} = \frac{1}{2} \sum_i m_i \dot{\mathbf{r}}_i \cdot \dot{\mathbf{r}}_i - \sum_{i>j} \phi(r_{ij}).$$

Andersen suggested that, for the (N,P,H) ensemble, we construct the Lagrangian

$$\mathcal{L}_2 = \frac{1}{2} \sum_i m_i L \dot{\boldsymbol{\rho}}_i \cdot L \dot{\boldsymbol{\rho}}_i - \sum_{i>j} \phi(L \rho_{ij}) + \frac{1}{2} C \dot{V}^2 - P_{\text{ex}} V,$$

In the case of an applied hydrostatic pressure, PR introduced the Lagrangian

$$\mathcal{L}_3 = \frac{1}{2} \sum_i m_i \dot{\mathbf{s}}_i^t G \dot{\mathbf{s}}_i - \sum_{i>j} \phi(r_{ij}) + \frac{1}{2} W \text{Tr}(\dot{\mathbf{h}}^t \dot{\mathbf{h}}) - P_{\text{ex}} V,$$

Constant Pressure MD for Molecular Solids

I now outline the equations of motion for a molecular solid (or liquid) using the (N,P,H) ensemble. In the following discussion the intermolecular interactions are represented by the sum of atom-atom (or site-site) contributions; however, the extension to handle more general forms of interaction is straightforward. The Lagrangian now takes the form (49, 50)

$$\begin{aligned} \mathcal{L}_4 = & \frac{1}{2} \sum_i m_i \dot{\mathbf{s}}_i^t G \dot{\mathbf{s}}_i + \frac{1}{2} \sum_i \omega_i I_i \omega_i \\ & + \frac{1}{2} W \text{Tr}(\dot{\mathbf{h}}^t \dot{\mathbf{h}}) - \sum_{i>j} \phi(r_{ij}, \mathbf{\Omega}_i, \mathbf{\Omega}_j) - P_{\text{ex}} V. \end{aligned}$$

The second term on the right-hand side is the rotational kinetic energy, I_i is the inertia tensor of molecule i , and ω_i is its angular velocity. The potential energy term has been formally modified to indicate that the intermolecular potential now depends on the molecular orientations $\mathbf{\Omega}$. An

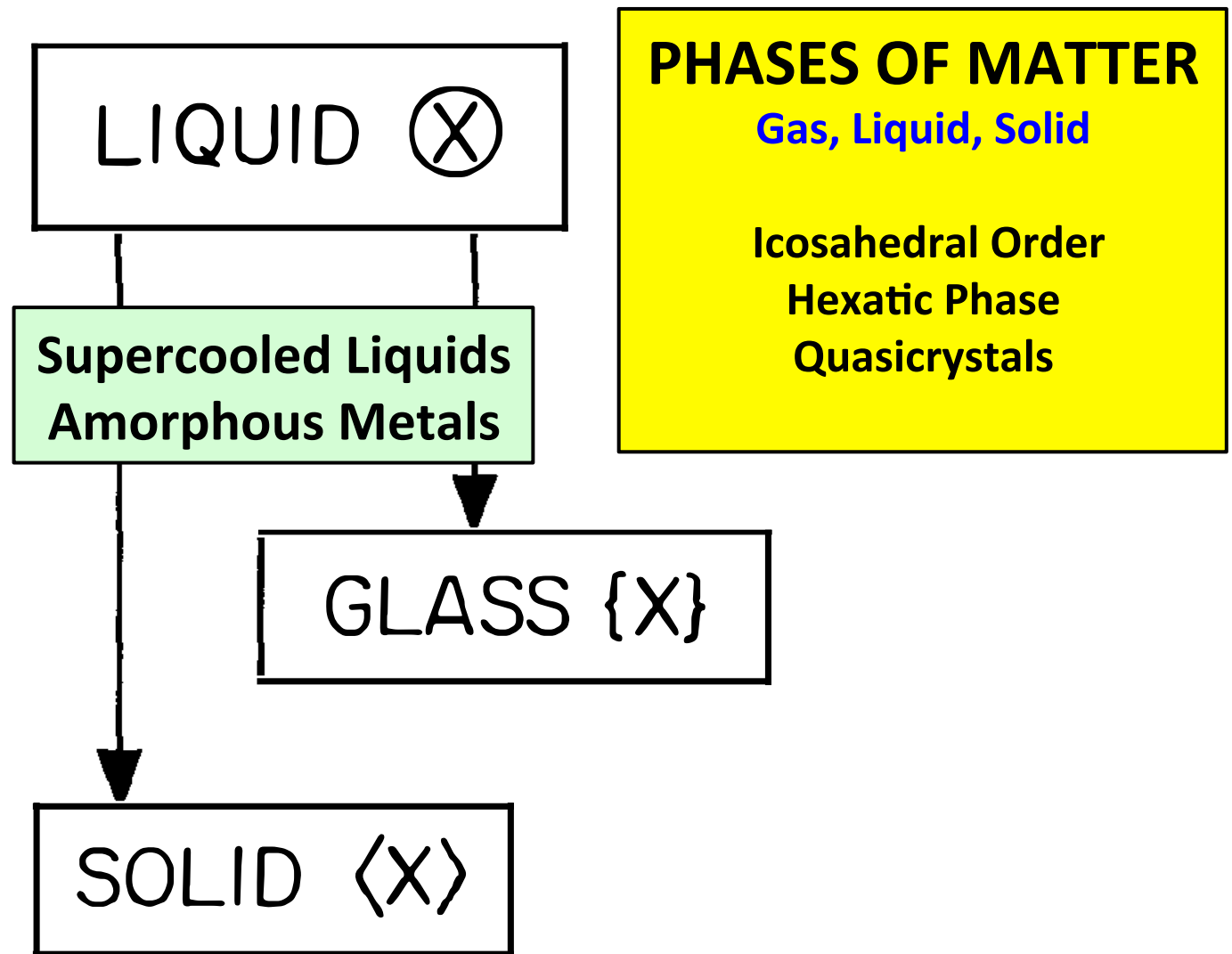


Figure 1 Schematic illustration of the result of quenching an atomic liquid. The atomic positions are denoted by the symbol X . Long-range translational order is denoted by the *brackets*, the lack of long-range order by *braces*, and the presence of translational diffusion the *circle*.

2D Melting – Hexatic Phase

Kosterlitz – Thouless – Nelson – Halperin – Young

Two transitions: First, when the solid undergoes a *dislocation* unbinding transition to the hexatic phase (short-range positional & quasi long-range orientational order). Second, is *disclination* unbinding that transforms the hexatic phase to an isotropic phase (short-range positional & orientational order).

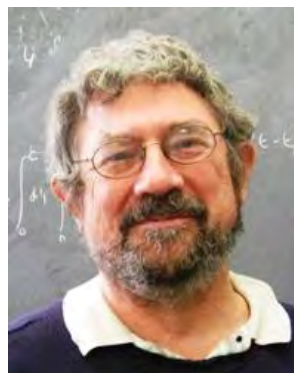
Ordering, metastability and phase transitions in 2D systems

J Michael Kosterlitz & David J Thouless

J. Phys. C (Solid State Physics) 6: 1181- (1973)



F. Duncan M. Haldane

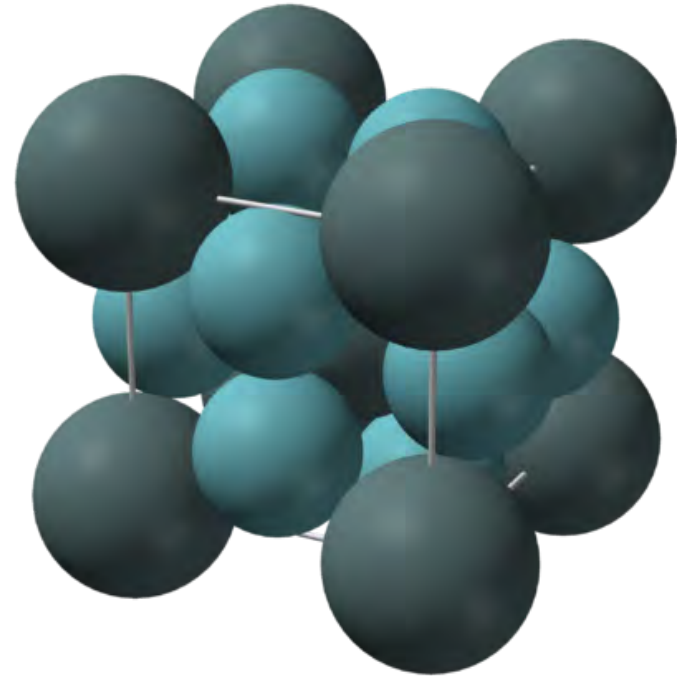


Nobel Prize Physics 2016: "for theoretical discoveries of topological phase transitions and topological phases of matter"

FRANK – KASPER PHASES



Unit cell of the A15
phase of Nb_3Sn



In 1958, Frank & Kasper introduced methodology to pack asymmetric icosahedra into crystals using other polyhedra with larger coordination numbers. These “coordination polyhedra” were constructed to maintain **topological close packing (TCP)** ..

[[wikipedia.org](https://en.wikipedia.org/wiki/Topological_close_packing)]

Sir F. Charles FRANK, FRS RS Copley Medal: "*fundamental contribution to the theory of crystal morphology, to the source of dislocations & their consequences in interfaces & crystal growth; to fundamental understanding of liquid crystals & the concept of disclination; and to the extension of crystallinity concepts to aperiodic crystals.*"



Acta Cryst. (1958). **11**, 184

Complex Alloy Structures Regarded as Sphere Packings. I. Definitions and Basic Principles

BY F. C. FRANK

H. H. Wills Physics Laboratory, University of Bristol, England

AND J. S. KASPER

Research Laboratory, General Electric Company, Schenectady, N.Y., U.S.A.

(Received 12 August 1957)

Complex alloy structures, particularly those of transition metals, are considered as determined by the geometrical requirements for sphere packing. A characteristic of the class of structures discussed is that tetrahedral groupings of atoms occur everywhere in the structure—alternatively stated, coordination polyhedra have only triangular faces. The topological and geometrical properties of such polyhedra are examined and rules and theorems regarding them are deduced. Justification is given for the prominence of four such polyhedra (for coordination numbers of 12, 14, 15 and 16) in actual structures. General principles regarding the combination of these polyhedra into full structures are deduced and necessary definitions are given for terms that facilitate the detailed discussion of this class of structures.



F. C. Frank, J. S. Kasper, Complex alloy structures regarded as sphere packings.

I. Definitions and basic principles. *Acta Crystallogr.* **11**, 184–190 (1958). doi:10.1107/S0365110X58000487;

II. Analysis and classification of representative structures. *Acta Crystallogr.* **12**, 483–499 (1959). doi:10.1107/S0365110X59001499

Complex Alloy Structures Regarded as Sphere Packings. II. Analysis and Classification of Representative Structures

BY F. C. FRANK

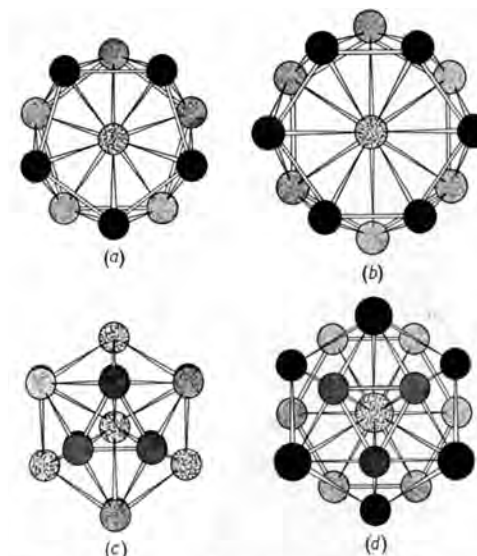
H. H. Wills Physical Laboratory, University of Bristol,

AND J. S. KASPER

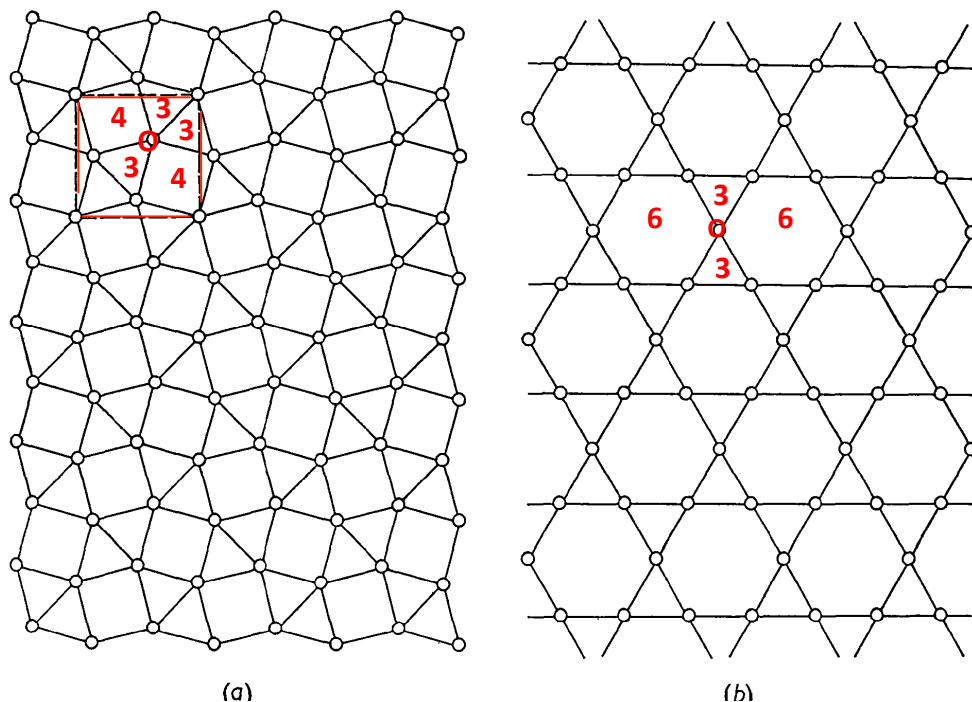
Research Laboratory, General Electric Company, Schenectady, New York, U.S.A.

(Received 29 September 1958)

The general principles and properties which have been deduced previously (Frank & Kasper, 1958) for the class of alloy structures with triangulated coordination polyhedra are applied in an analysis and classification of representative structures. In the main the analysis is with regard to the nature of layers and how they may be stacked and with regard to the nature of the major skeletons. Many hypothetical structures resulting from the analysis are listed and procedures are given for predicting other structure types. The relationship between alloy structures and inert gas hydrates is discussed.



Coordination Polyhedra:
 (a) Icosahedron, CN 12
 (b) CN 14 (c) CN 15 (d) CN 16



The two basic nets in complex alloy structures:
 (a) $3^2, 4, 3, 4$ net;
 (b) Kagomé net $3, 6, 3, 6$.
 Numerical symbols are number & sequence of polygons around each vertex.

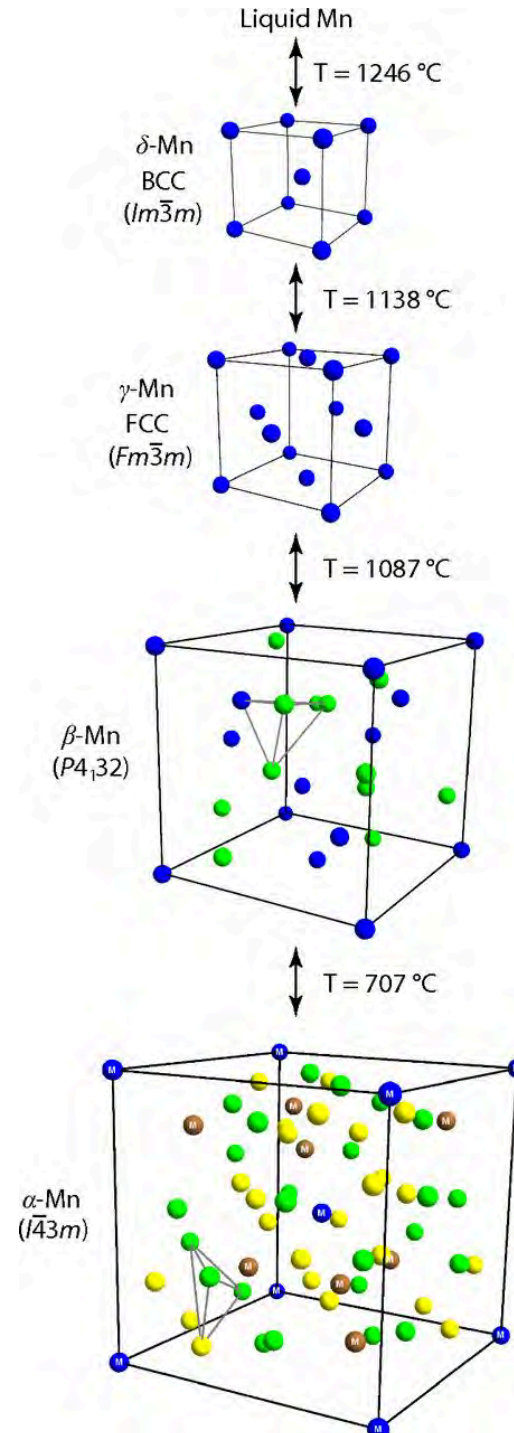


Q: Why do atoms pack in such diverse structures ?

Crystal Phases of Manganese

On cooling the liquid the sequence includes:

δ -Mn (BCC),
 γ -Mn (FCC),
 β -Mn ($P4_132$),
 α -Mn



ALPHA MANGANESE AND THE FRANK KASPER PHASES

Scripta METALLURGICA Vol. 19, pp. 535-538, 1985

R. E. Watson

Brookhaven National Laboratory[†], Upton, N. Y. 11973

L. H. Bennett

National Bureau of Standards, Gaithersburg, Md. 20899

Transition metal alloys often form in a group of structures, known as **topologically-close-packed, TCP**, systems. The TCP phases, which include the σ , Al₅ and Laves systems, form in brittle complex structures. **Frank & Kasper** defined the TCP systems by considering the packing of twelve and higher-fold triangulated coordination polyhedra, the higher-fold ones involving negative disclinations ("*major ligands*" in Frank-Kasper notation). Frank & Kasper considered the crystal structures allowed subject to two principles: that lines of disclinations extend all the way across the crystal and that planar atomic layers containing certain patterns occur. The Frank-Kasper polyhedra, which arise are the (0,0,12), (0,0,12,2), (0,0,12,3) and (0,0,12,4), i.e., there is no thirteen-fold polyhedron since it would appear that a disclination would have to halt at such a site. Frank & Kasper catalogued a number of structures. *There is a problem with the α -Mn structure since there are Mn^{III} sites with not-allowed 13-fold, as well as other sites with allowed 12 & 16-fold coordination.*

Pearson has noted that the Mn^{III} sites have a 14th neighbor at a distance intermediate between the first and second shells of neighbors and suggested that the Mn^{III} might lie at a severely distorted Frank-Kasper (0,0,12,2) site.



Quasi Crystals: **Dan Shechtman** first observed ten-fold diffraction patterns of Al/Mn alloys in 1982. Publication came later: “**The microstructure of rapidly solidified Al₆Mn**” *Metallurgical Transactions* 16 (6): 1005-1012 (1985)
Nobel Prize in Chemistry 2011



D. Schectman & I. Blech:

The microstructure of rapidly solidified Al–Mn alloys containing 18 - 25.3 wt % Mn was studied by TEM. One of the phases found exhibits icosahedral symmetry manifested in electron diffraction patterns having **five-fold symmetry**. A new structural concept is proposed to account for the observed electron diffraction patterns. The structure is assumed to be composed of many connected polyhedra. Although not forming a regular lattice, such structures are able to produce sharp diffraction peaks. The terminal stability and transformation of the icosahedral phase was also studied and reported.



Metallic Phase with Long-Range Orientational Order and No Translational Symmetry

D. Shechtman and I. Blech

Department of Materials Engineering, Israel Institute of Technology-Technion, 3200 Haifa, Israel

and

D. Gratias

Centre d'Etudes de Chimie Métallurgique, Centre National de la Recherche Scientifique, F-94400 Vitry, France

and

J. W. Cahn

Center for Materials Science, National Bureau of Standards, Gaithersburg, Maryland 20760

(Received 9 October 1984)

We have observed a metallic solid (Al-14-at.-%-Mn) with long-range orientational order, but with icosahedral point group symmetry, which is inconsistent with lattice translations. Its diffraction spots are as sharp as those of crystals but cannot be indexed to any Bravais lattice. The solid is metastable and forms from the melt by a first-order transition.

Quasicrystals: A New Class of Ordered Structures

Dov Levine

Department of Physics, University of Pennsylvania, Philadelphia, Pennsylvania 19104

and

Paul Joseph Steinhardt

Department of Physics, University of Pennsylvania, Philadelphia, Pennsylvania 19104,

and IBM Thomas J. Watson Research Laboratory,

Yorktown Heights, New York 10598

(Received 2 November 1984)

A quasicrystal is the natural extension of the notion of a crystal to structures with quasi-periodic, rather than periodic, translational order. We classify two- and three-dimensional quasicrystals by their symmetry under rotation and show that many disallowed crystal symmetries are allowed quasicrystal symmetries. We analytically compute the diffraction pattern of an ideal quasicrystal and show that the recently observed electron-diffraction pattern of an Al-Mn alloy is closely related to that of an icosahedral quasicrystal.



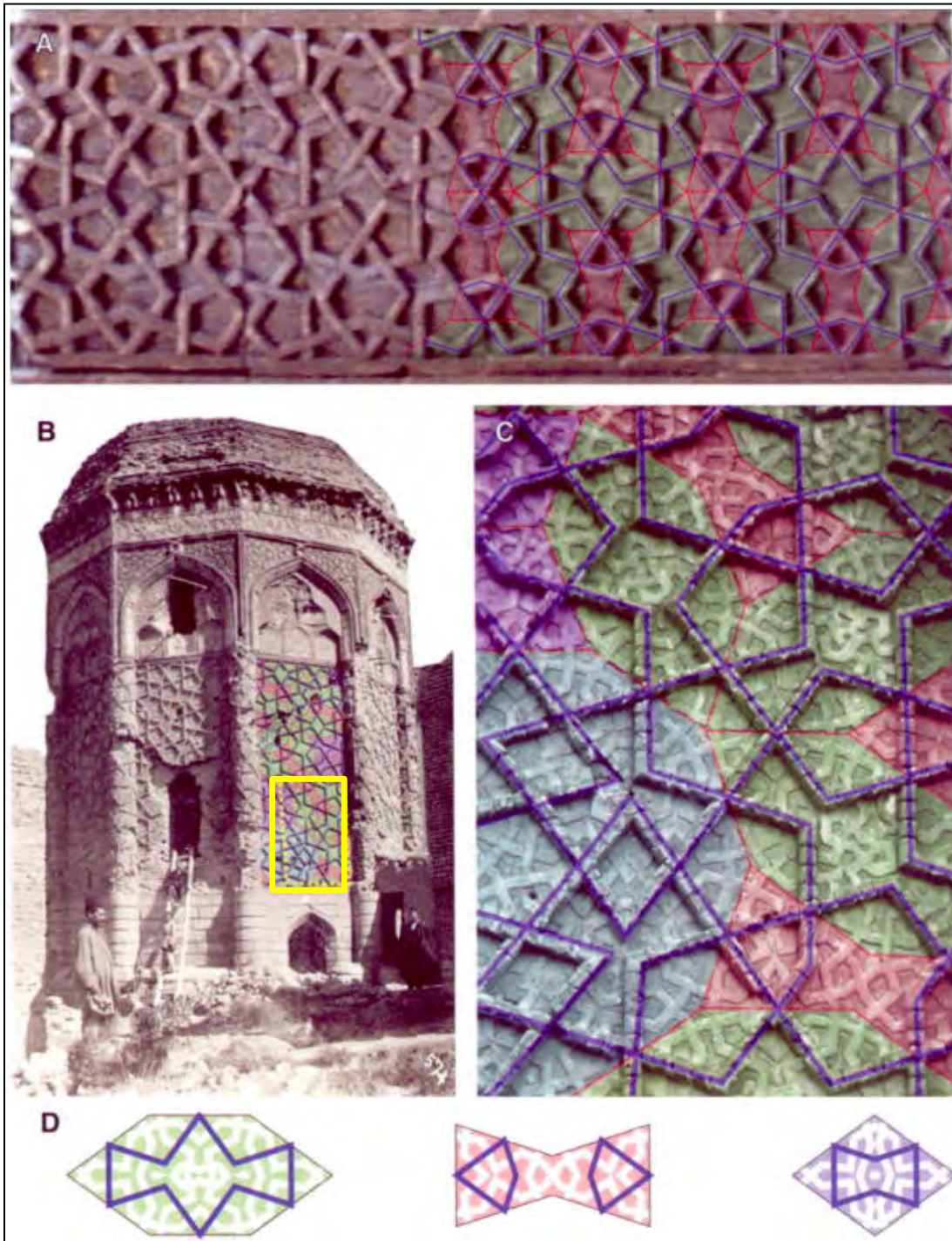
Decagonal and Quasi-Crystalline Tilings in Medieval Islamic Architecture

Peter Lu & Paul J. Steinhardt

Science **315**(5815): 1106-1110 (2007)

The conventional view holds that geometric star-and-polygon, or strapwork patterns (girih) in medieval Islamic architecture were conceived by their designers as a network of zigzagging lines, where the lines were drafted directly with a straightedge and a compass.

We show that by 1200 C.E. a conceptual breakthrough occurred in which girih patterns were reconceived as tessellations of a special set of equilateral polygons ("girih tiles") decorated with lines. These tiles enabled the creation of increasingly complex periodic girih patterns, and by the 15th century, the tessellation approach was combined with self-similar transformations to construct nearly perfect quasi-crystal Penrose patterns, five centuries before their discovery in the West.

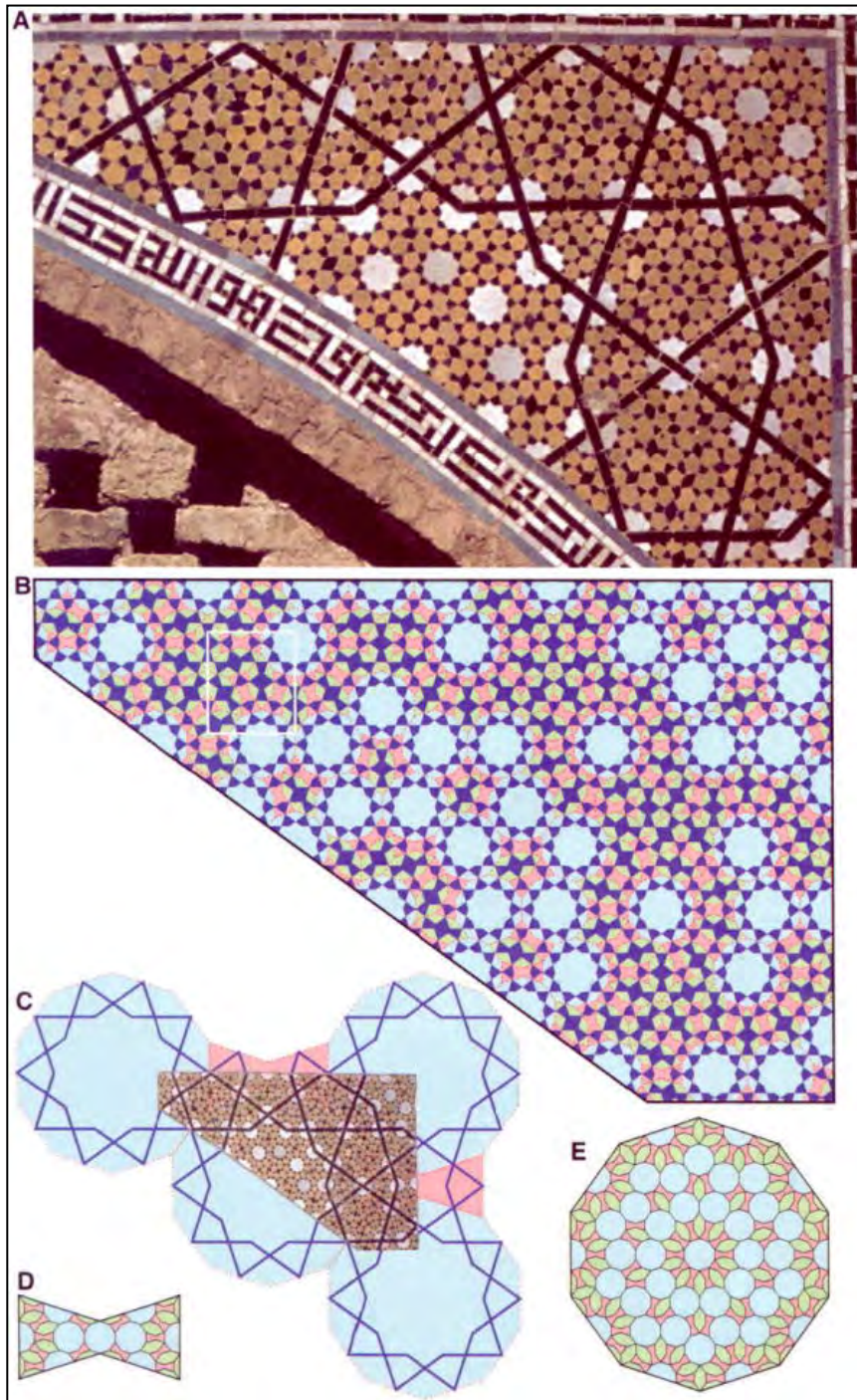


(A) Periodic girih pattern from the Seljuk Mama Hatun Mausoleum in Tercan, Turkey (~1200 C.E.), where all lines are parallel to the sides of a regular pentagon, even though no decagon star is present; reconstruction overlaid at right with the hexagon and bowtie girih tiles.

(B) Photograph [A. Sevruguin 1870s] of the octagonal Gunbad-i Kabud tomb tower in Maragha, Iran (1197 C.E.), with the girih-tile reconstruction of one panel overlaid.

(C) Close-up of the area marked by the yellow rectangle in (B).

(D) **Hexagon**, **bowtie**, and **rhombus** girih tiles with additional small-brick pattern reconstruction (indicated in white) that conforms not to the pentagonal geometry of the overall pattern, but to the internal two-fold rotational symmetry of the individual girih tiles.

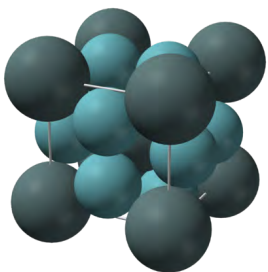


Girih-tile subdivision found in the decagonal girih pattern on a spandrel from Darb-i Imam shrine, Isfahan, Iran (1453 C.E.). (A) Photograph of the right half of the spandrel. (B) Reconstruction of the smaller-scale pattern using girih tiles. (C) Reconstruction of the larger-scale thick line pattern with larger girih tiles, overlaid on the building photograph. (D, E) Graphical depiction of the subdivision rules transforming the large **bowtie** (D) and **decagon** (E) girih-tile pattern into the small girih-tile pattern on tilings from the Darb-i Imam shrine and Friday Mosque of Isfahan.

**FRANK-KASPER PHASES
DEVELOPED FOR ATOMIC
ALLOYS BUT WHAT ABOUT
MOLECULES ..?**

SOLID OXYGEN

Solid/Liquid Oxygen has clear/light blue color. Melting point is 54.4K



**FRANK – KASPER
A15 PHASE (A₃B)**

**8 molecules (1-8):
2 “spheres” (1,8)
6 “disks” (2-7)**

γ -O₂ Pm 3n

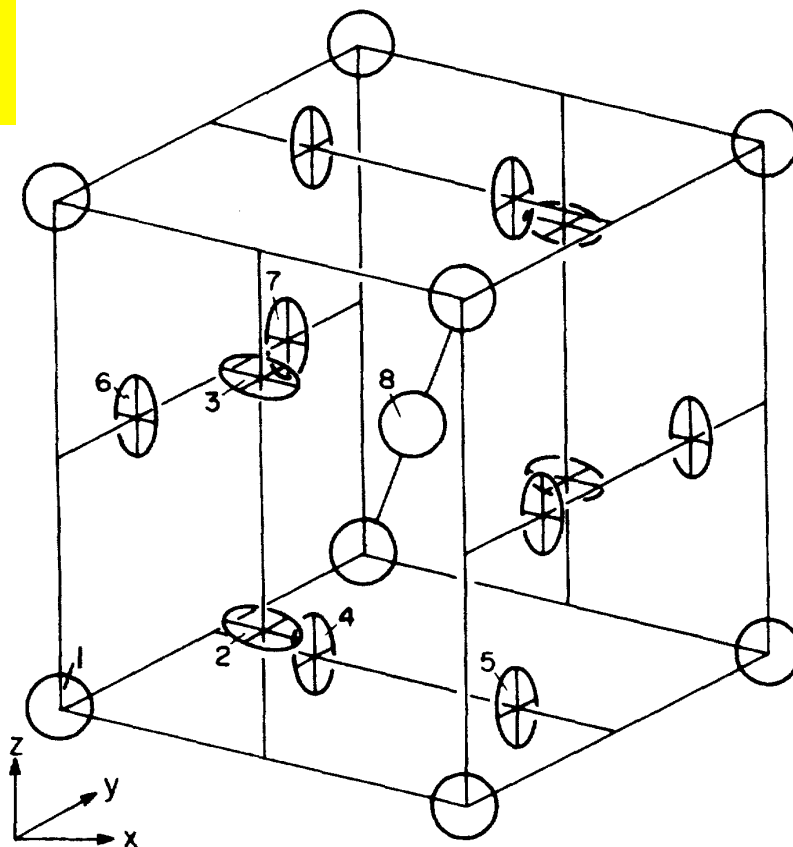
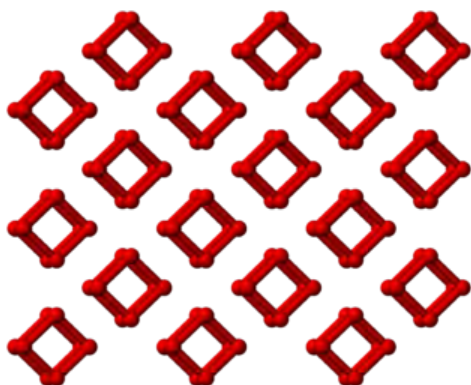


FIG. 1. The crystal structure of γ -O₂. The “disk-like” molecules (2–6) have site symmetry D_{2d} , while the “spherical” molecules (1, 8) have site symmetry T_h and are preferentially oriented in $\langle 111 \rangle$ directions.



Molecular-dynamics study of solid γ -O₂

Michael L. Klein

Chemistry Division, National Research Council of Canada, Ottawa, Canada K1A 0R6

D. Levesque and J.-J. Weis

Laboratoire de Physique Théorique et Hautes Energies, Université Paris-Sud, 91405 Orsay, France*

(Received 4 February 1980)

Published online 13 September 2006 | Nature | doi:10.1038/news060911-7

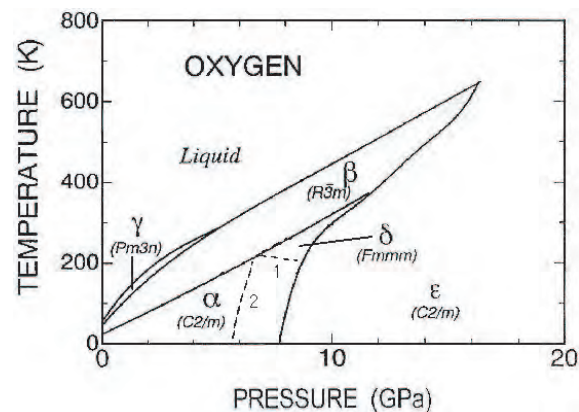
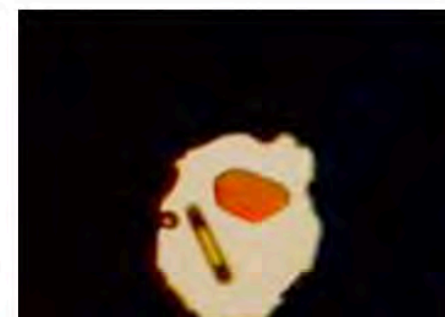
News

Just a pretty phase?

Solid red oxygen: useless but delightful.

Richard Van Noorden

Scientists have revealed the crystal structure of a dark red form of solid oxygen that forms at immense pressures. The results are surprising, elegant — and entirely useless. But the high-pressure techniques used to make the crystal could soon find applications.



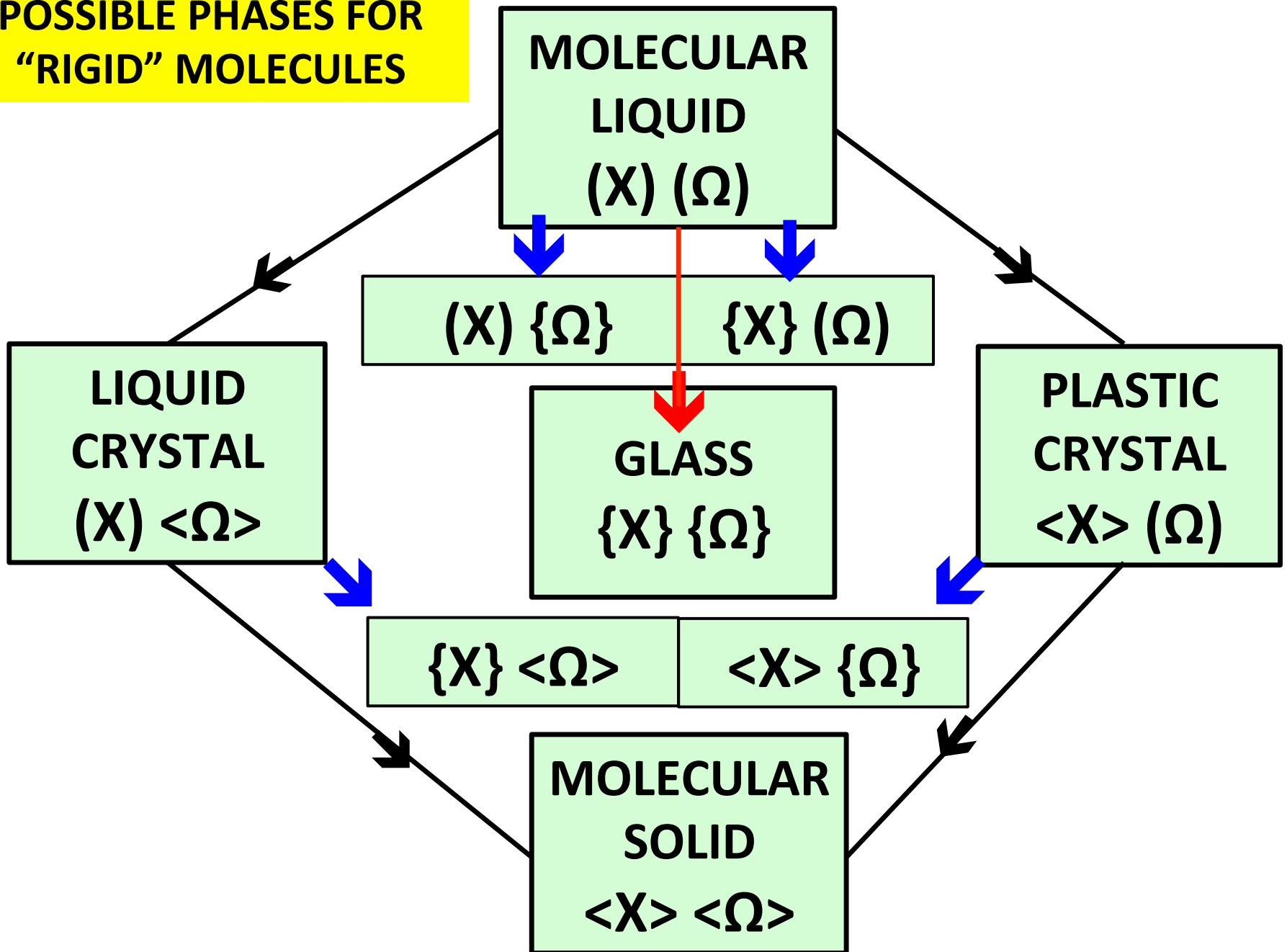
α -phase: *light blue* — monoclinic $T < 23.8\text{K}$ at 1 atm below 23.8 K
 β -phase: *faint blue to pink* — forms at 1 atm below 43.8 K, rhombohedral
 γ -phase: *faint blue* — forms at 1 atm below 54.36 K, cubic structure
 δ -phase: *orange* — room temperature by applying 9 GPa pressure
 ϵ -phase: *dark-red to black* — room temperature at pressures > 10 GPa
 ζ -phase: *metallic* — forms at pressures greater than 96 GPa

**SOLID
OXYGEN**

**WHAT ABOUT OTHER
MOLECULES ..?**

**POTENTIALLY MANY POSSIBILITIES
FOR DISORDERED PHASES ..**

**POSSIBLE PHASES FOR
"RIGID" MOLECULES**



CH₃OH

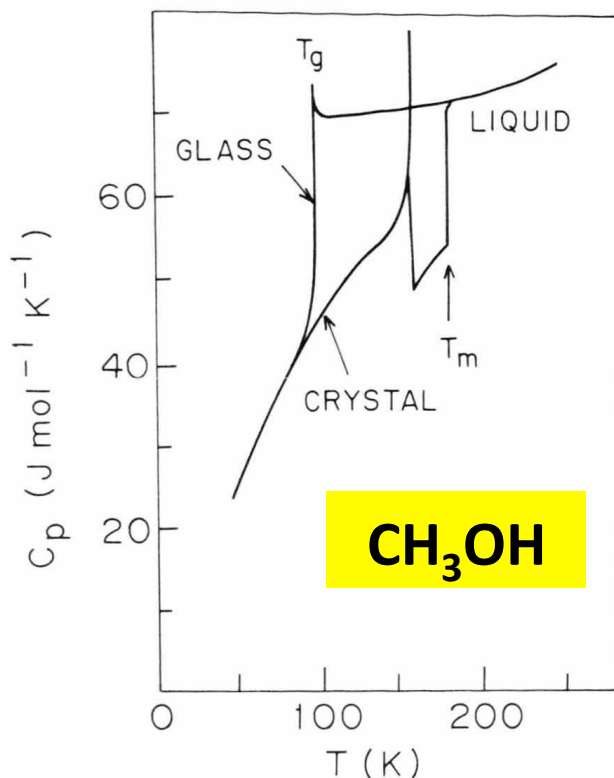


Fig. 2. Experimental temperature variation of the heat capacity of methanol taken from [14]. The solid–solid phase transition at around 160 K and the melting point, T_m , should be distinguished from the glass transition, $T_g = 103$ K.

Other MD simulations used to test mode coupling theory ..

A Computer Simulation Study of Supercooled Liquid and Amorphous-Solid Methanol

Massimo Marchi *

Department of Chemistry, McMaster University, Hamilton, Ontario, Canada L8S 4M1

Michael L. Klein

Department of Chemistry, University of Pennsylvania, Philadelphia, Pennsylvania, USA 19104-6323

Z. Naturforsch. **44a**, 585–590 (1989); received April 12, 1989

Dedicated to Professor Jacob Bigeleisen on the Occasion of his 70th Birthday

The constant-pressure molecular dynamics technique has been used to study the structural consequences of cooling liquid methanol. We employed a periodically replicated system of 250 molecules interacting with an intermolecular potential fitted to thermodynamic properties of the liquid. Plots of the enthalpy and volume against temperature exhibit a distinct change in slope around 160 K; a feature that is identified with the onset of structural arrest, occurring on the picosecond time-scale, in the supercooled liquid. The corresponding glass transition in real methanol occurs around 103 K. The main structural feature that accompanies the structural arrest is the appearance of a splitting in the primary peak of the radial distribution function for methyl groups. This observation contrasts strongly with the behaviour of atomic systems where such splittings arise only in the second peaks of distribution functions. The calculations are discussed in the light of recent neutron scattering data on glassy methanol.

S. Yashonath & C.N.R. Rao Monte Carlo Simulation of Isopentane Glass *Proc. Roy. Soc. London A 400, 61 (1985)*



Carbon Tetrachloride, CCl₄

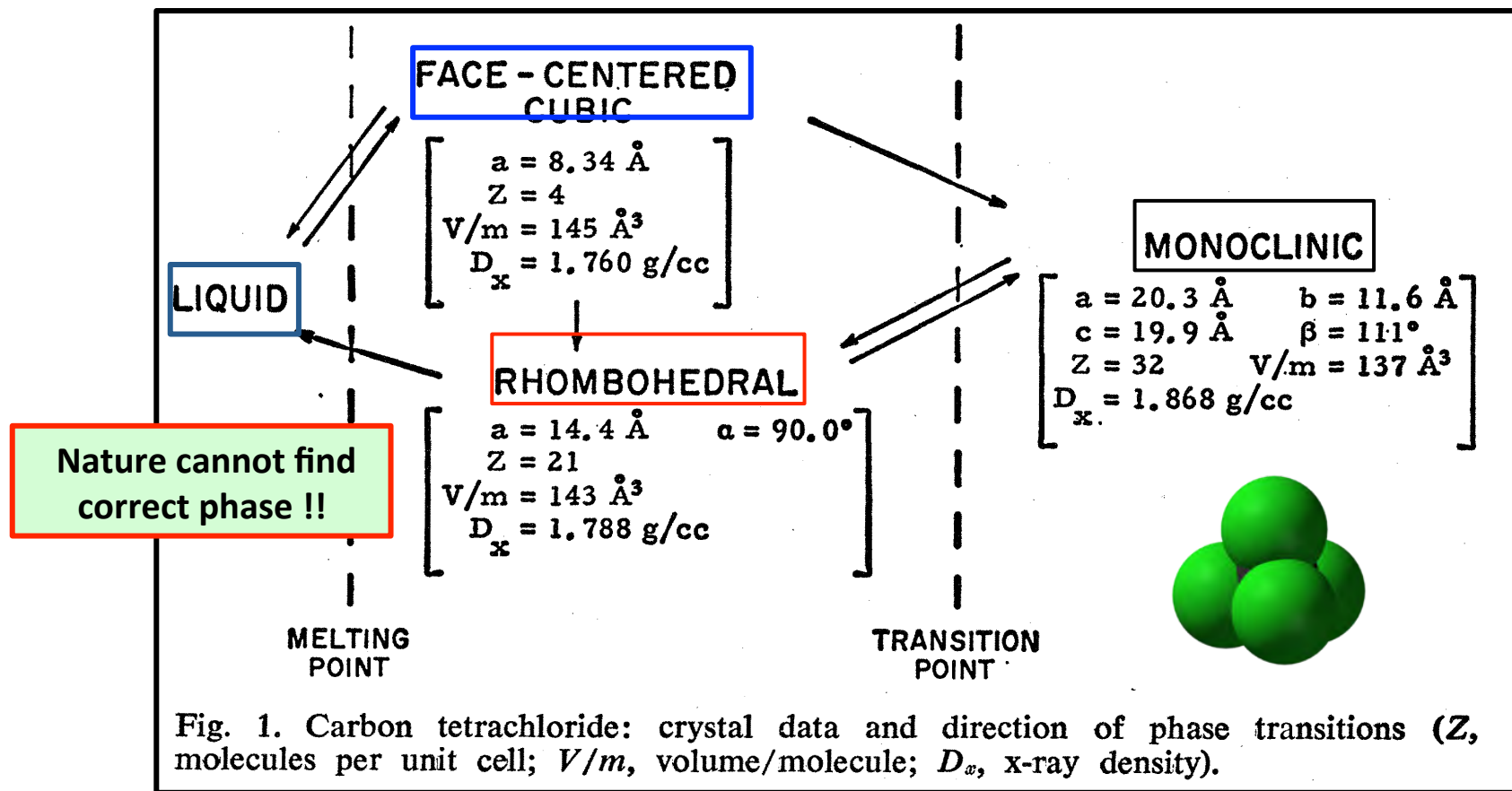
**Freezes into FCC orientationally
disordered “plastic” phase**



Carbon Tetrachloride: A New Crystalline Modification

Ruben Rudman & Ben Post *Science* **154** (3752): 1009 (1966)

Abstract. *X-ray and optical studies of single crystals of carbon tetrachloride have established the existence of a previously unreported rhombohedral modification stable between the melting point and the transition temperature. The discovery of this phase emphasizes the need for a careful reinterpretation of available measurements of the thermal properties of solid carbon tetrachloride.*



The dual melting curves and metastability of carbon tetrachloride

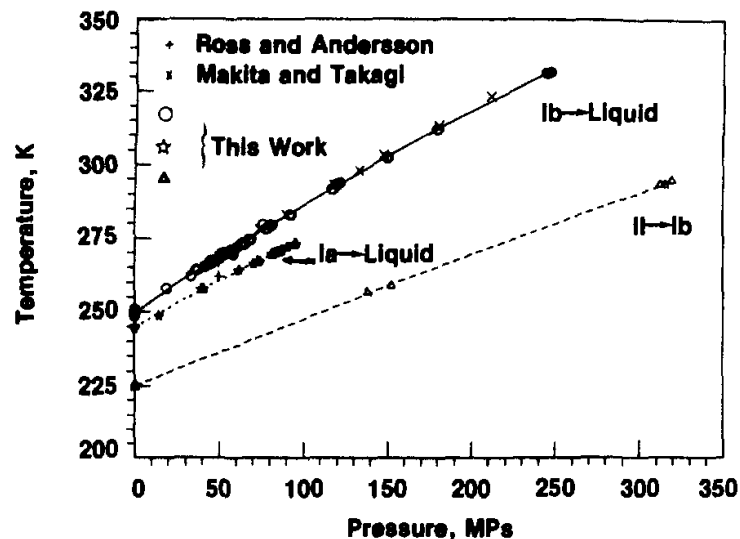
J. Chem. Phys. 72, 5838 (1980); <http://dx.doi.org/10.1063/1.439107>

Vern E. Bean and Sharrill D. Wood

National Bureau of Standards, Washington, D.C. 20234

(Received 21 December 1979; accepted 19 February 1980)

Carbon tetrachloride has three known solid phases at atmospheric pressure: Ia (face-centered cubic), Ib (rhombohedral), and II (monoclinic). Both Ia and Ib melt directly at temperatures some 5 K apart. These phase changes have been traced as a function of hydrostatic pressure up to 350 MPa. Between atmospheric pressure and 100 MPa, CCl₄ has dual melting curves; one for Ia, and a few degrees higher, one for Ib. The two curves diverge with increasing pressure. Above 100 MPa it was not possible to detect the Ia phase. There appears to be no Ia-Ib-liquid triple point. The metastability associated with these phases is discussed.

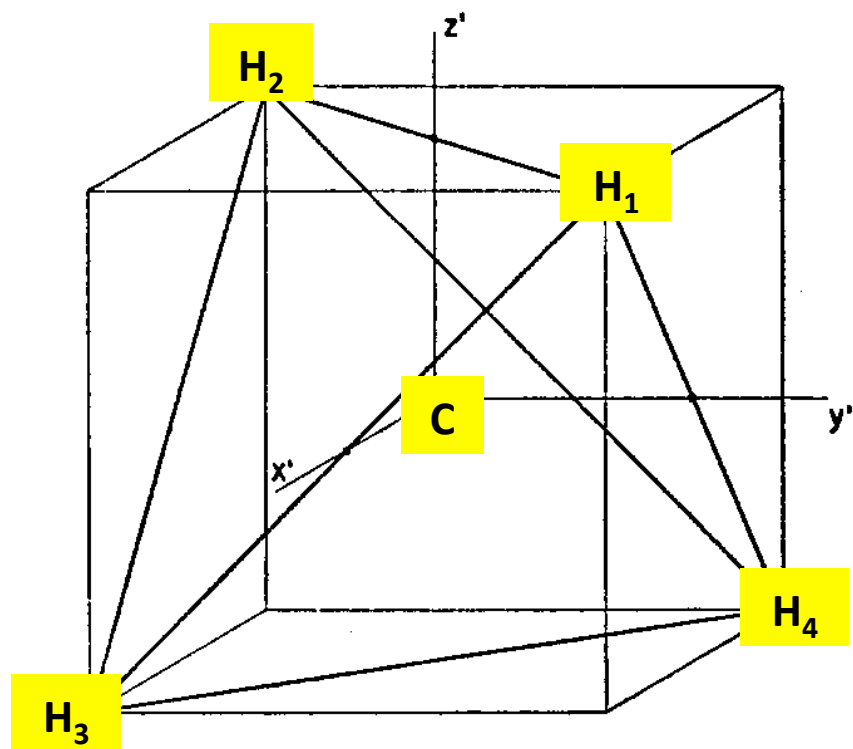


Note: $\Delta T_m = 5 \text{ K}$

FIG. 2. Curves for the Ib → liquid, Ia → liquid, and II → Ib transitions.

**ANOTHER EXAMPLE
METHANE, CH₄**

**Freezes into FCC orientationally
disordered “plastic” phase**



**CHARGE DISTRIBUTION
C-H BOND POLARITY**

FIG. 4. Coordinate system fixed in molecule. The charge distribution of the molecule has the same elements of symmetry as the indicated tetrahedron.

METHANE HAS AN OCTOPOLE MOMENT
 $\langle \psi_0 | \Omega_{\alpha\beta\gamma} | \psi_0 \rangle$

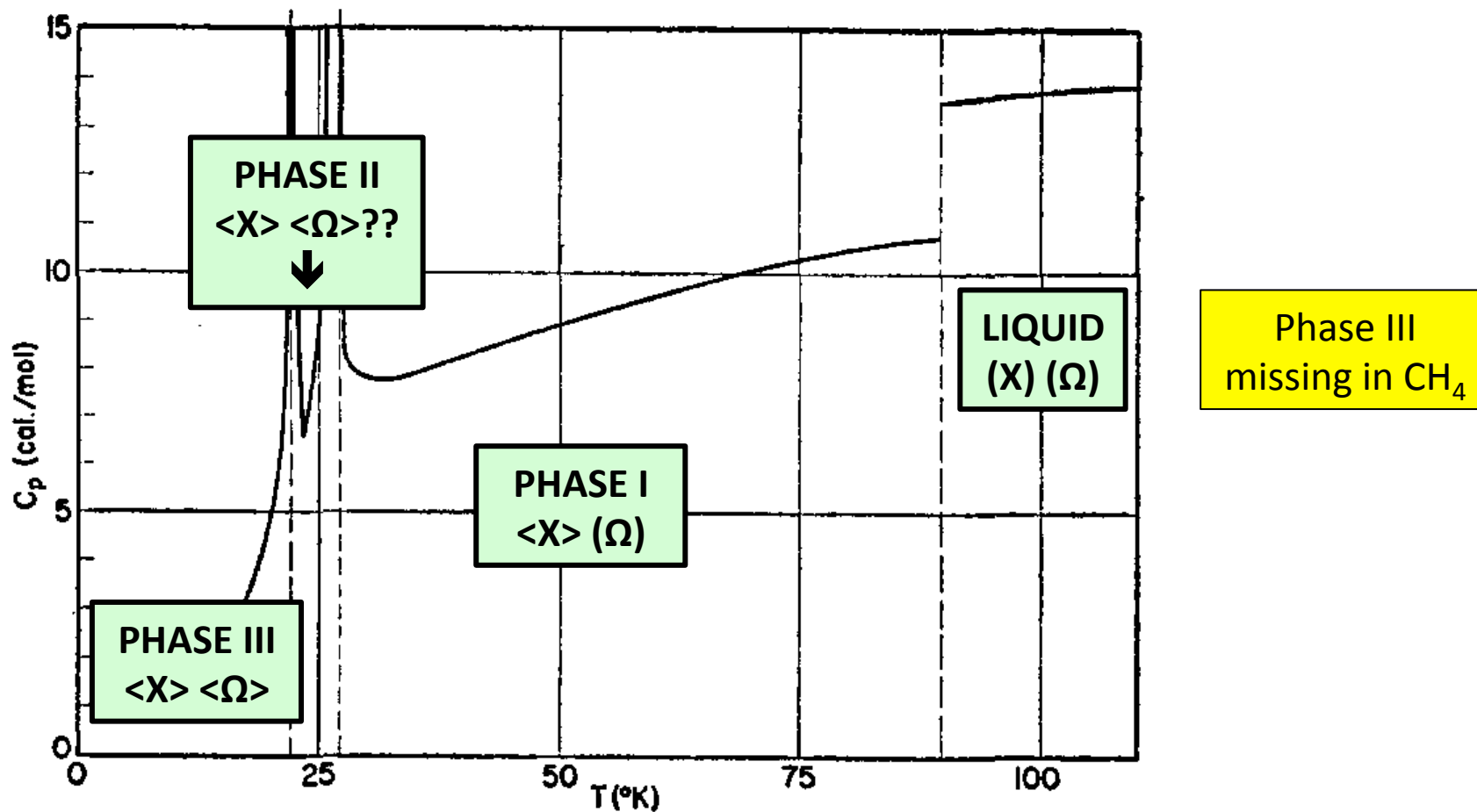


FIG. 1. Specific heat of CD_4 . Melting occurs at $89.8^\circ K$. Data of K. Clusius and L. Popp, reference 8.

METHANE CONDENSED PHASES

Theory of Phase Transitions in Solid Heavy Methane*

HUBERT M. JAMES AND THOMAS A. KEENAN†

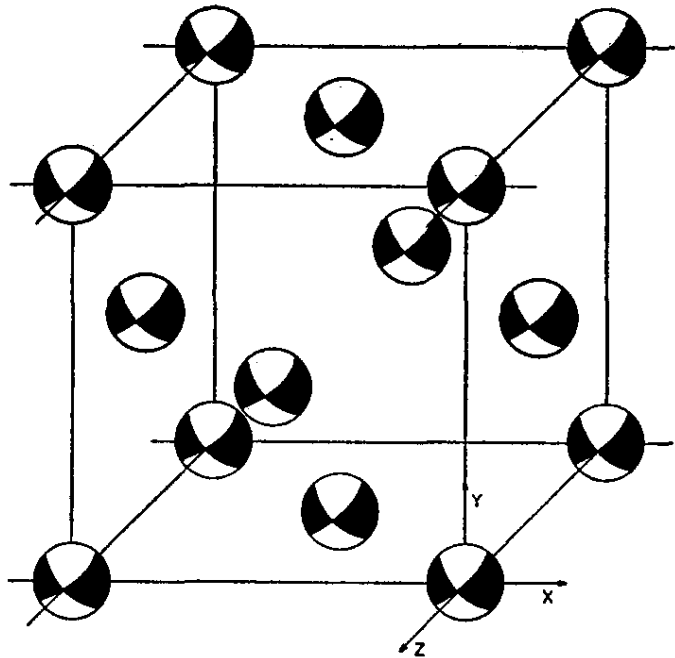
Purdue University, West Lafayette, Indiana

(Received December 18, 1958)

It is the purpose of this paper to explain the existence of three solid phases in CD_4 , and to predict the molecular ordering in each phase, by straightforward deduction from a reasonable assumption concerning the orientational coupling of the molecules. Molecular and lattice vibrations are neglected, the crystal being treated as an f.c.c. array of spherical rotators carrying distributions of charge with tetrahedral symmetry. It is assumed that the dominant term in the orientational coupling of the molecules is their electrostatic interaction, of which only the octopole-octopole interaction of next neighbors is retained in the calculation. The magnitude of the effective octopole moment is the only disposable constant in the theory. The statistical calculation is based on a classical version of the self-consistent field idea; neglect of quantum effects makes the results inapplicable to CH_4 , which shows large isotope differences from CD_4 . The conditions for self-consistency in the theory appear as a family of integro-functional equations, one for each molecule in the crystal. These are brought into convenient form by introduction of tetrahedral harmonics and associated tetrahedral rotator functions. The consistency equations are first solved for the cases in which the orientational distribution function is the same for all molecules in the crystal. There exist three distinct solutions of this type, in which all molecules are subject to identical orienting fields with symmetries T , C_2 , or D_3 , respectively. More general solutions are

then found, for which the molecules are not all equivalent, but may be freely rotating, or in orienting fields of symmetry T , C_2 , or D_3 . The consistency relations state restrictions on the distribution of such molecules in the crystal lattice, and fix the strengths of the orienting fields; they can be satisfied only for small numbers of molecules in a crystal cell. An apparently exhaustive tabulation is made of all solutions with low free energy. Three of these minimize F in some temperature range, and describe stable phases. At the lowest temperatures the stable phase has tetragonal symmetry V_d , with all molecules oscillating about equivalent equilibrium orientations. As T rises this undergoes a first-order transformation to a phase with octahedral symmetry O , in which one molecule in four rotates freely, surrounded by a shell of oscillating next neighbors. At higher temperatures this undergoes a transformation (described by the theory as of second order) to an orientationally disordered phase. If the molecular octopole moment is assigned the magnitude 0.504×10^{-21} electron cm^3 needed to make the predicted upper transition temperature agree with the 27.1°K observed in CD_4 , the predicted lower transition temperature is 24.4°K , as against the observed 22.2°K . Predictions of the theory are also in satisfactory agreement with observations on integrated heats of transition, zero-point entropy, and the optical properties of the phases.

SEMINAL WORK ON PHASE TRANSITIONS



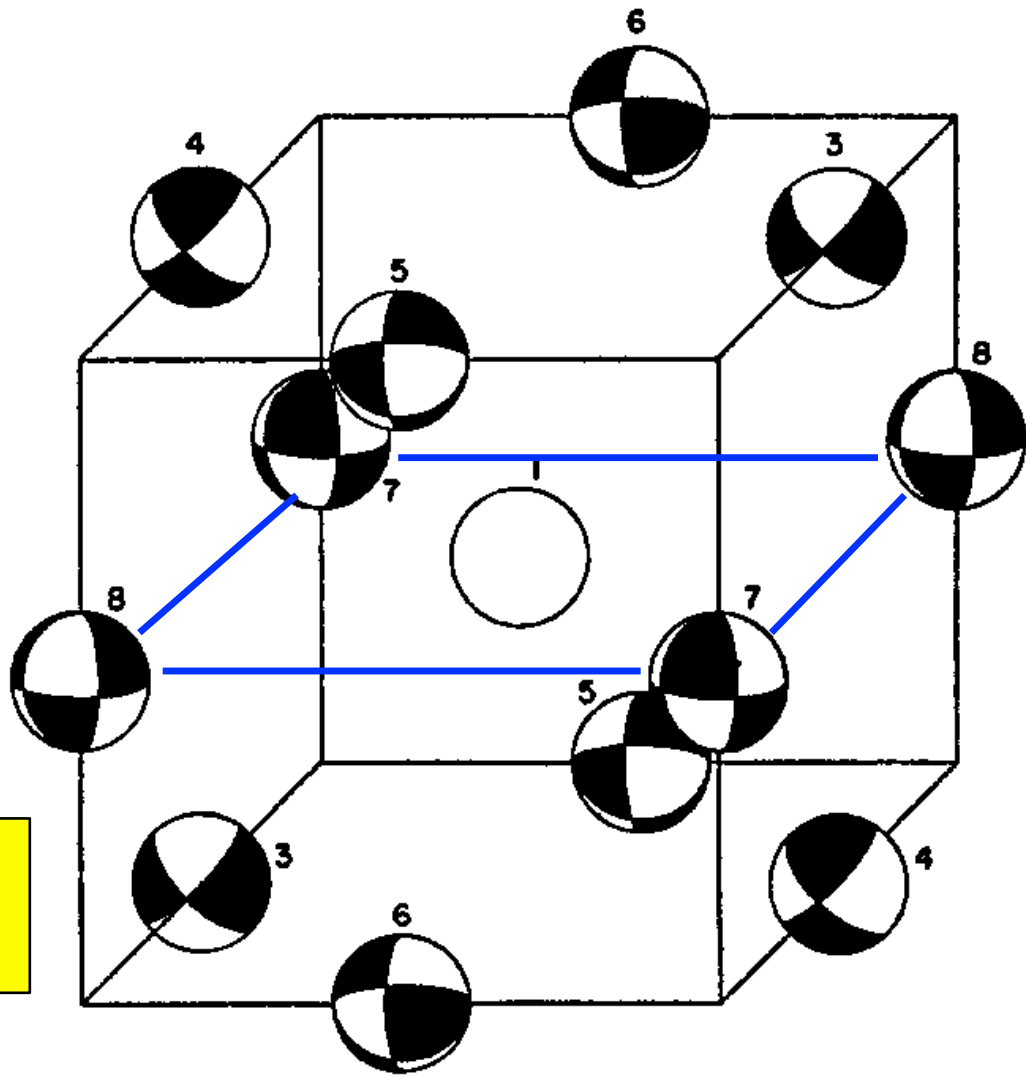
**PHASE I = FCC
ROTATOR PHASE
NMR & X-RAYS**

**PREDICTED GROUND
STATE OF SOLID CD_4**

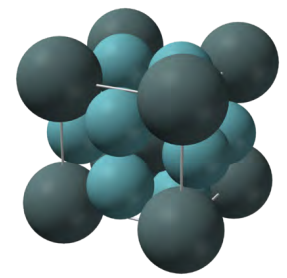
(1) the tetragonal Phase III, stable at the lowest temperatures,

(2) the octahedral Phase II, which becomes stable at a temperature below T_b , and persists up to $T = T_c$,

(3) the orientationally disordered Phase I,



8 molecules (1-8):
 2 disordered (1,2)
 6 ordered (3-8)



**JAMES & KEENAN
 (1959) PREDICTED
 PHASE II SOLID CD₄**

**A₃B but FCC not
 FRANK – KASPER
 A15 PHASE (BCC+..)**

Structure & Phase Transitions of Solid Heavy Methane (CD₄)

Werner Press J. Chem. Phys. 56, 2597 (1972); <http://dx.doi.org/10.1063/1.1677586>

The orientational structures and the phase transitions (27.0 and 22.1°K) of solid CD₄ are investigated by coherent neutron scattering from powder samples as well as from single crystals. In its **high temperature Phase I** CD₄ is found to crystallize within the space group **Fm3m with four molecules per unit cell** and a lattice constant $a_0=5.96 \text{ \AA}$ at 77°K. The molecular orientations are completely disordered at 35°K, while an indication of partial order was detected at 77°K. The transition to phase II is accompanied by critical fluctuations with a correlation length of about 24 Å (at 27.7°K) and appears to be of second order (critical exponent $\beta = 0.4 \pm 0.1$). **In Phase II six of eight molecules order with a local symmetry 42m, while the remaining two are orientationally disordered.** The space group is cubic *Fm3c* with 32 molecules per unit cell and $a_0=11.64 \text{ \AA}$ at 24.5°K. The transition to **Phase III** is predominantly of first order. With the present data the structure of phase III cannot be determined unambiguously. Superlattice reflections can be indexed cubic primitive. The number of molecules per unit cell remains 32, with $a_0=11.61 \text{ \AA}$ at 17.5°K. *The data suggest, that the low temperature structure is to be understood by an ordering within the sublattices of molecules disordered in phase II together with slight distortions of the other sublattices.* The structures of **Phases I and II agree** with the ones predicted by **James & Keenan** under the assumption of octupole—octupole interaction between nearest neighbor molecules. For **Phase III** the model of James & Keenan, as well as other predictions, hitherto published, must be ruled out.

Maximizing Entropy by Minimizing Area: Towards a New Principle of Self-Organization

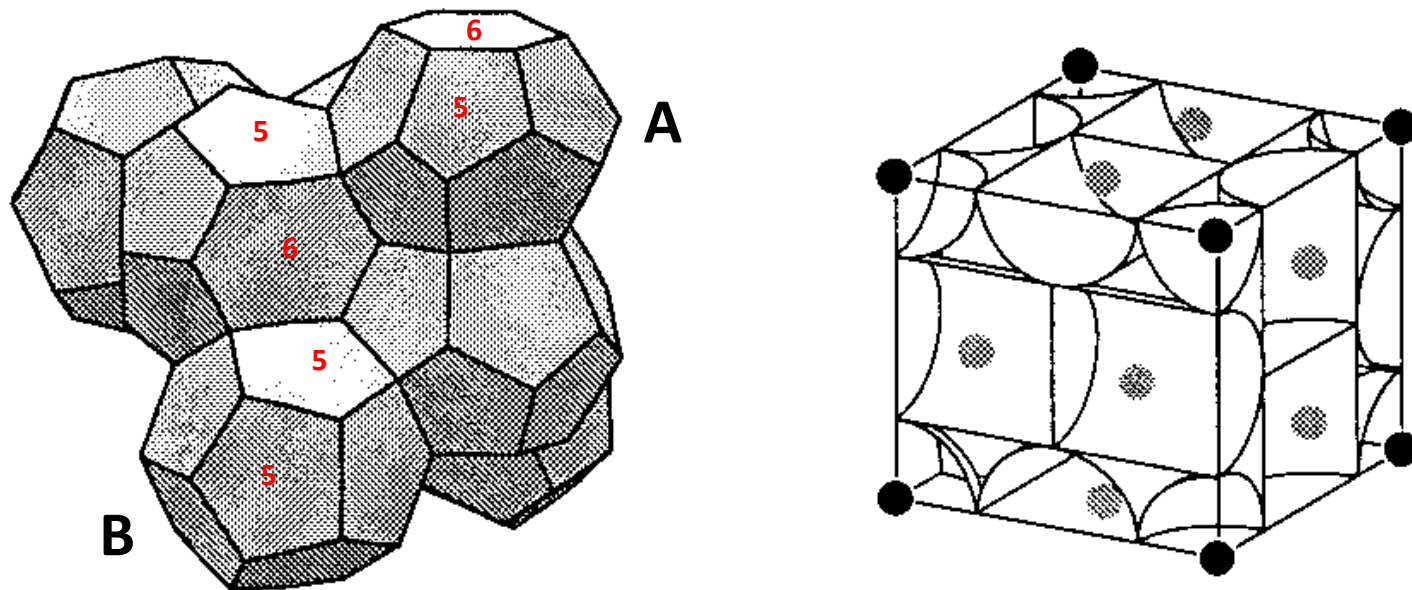
[P. Ziherl & Randall D. Kamien](#)

J. Phys. Chem. B **105** (42): 10147–10158 (2001);

DOI: 10.1021/jp010944q

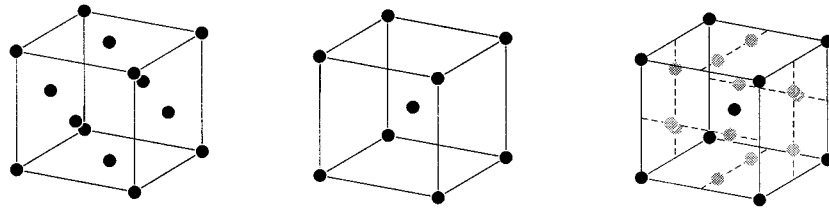


We propose a heuristic explanation for the numerous non-close-packed crystal structures observed in various colloidal systems. By developing an analogy between soap froths and the soft coronas of fuzzy colloids, we provide a geometrical interpretation of the free energy of soft spheres. We show that the close-packing rule associated with hard-core interactions and positional entropy of particles is frustrated by a minimum-area principle associated with the soft tail and internal entropy of the soft coronas ... **the A15 lattice, known to be area minimizing, is favored for a reasonable range of model parameters and so it is among the possible equilibrium states for a variety of colloidal systems.**

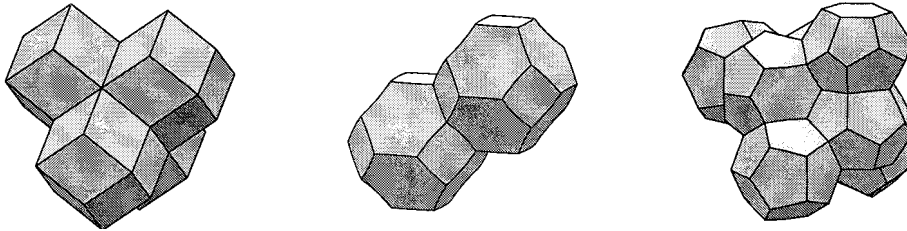


The **A15 foam** consists of **six** Goldberg **tetrakaidecahedra**, each with **two hexagonal and 12 pentagonal faces** (A), which form three sets of interlocking columns, and **two** irregular **pentagonal dodecahedra** (B) at the interstices.

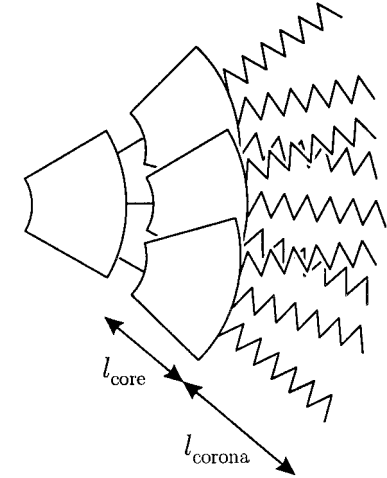
Approximate analytical model of the bulk free energy for the A15 lattice. Free volumes of columnar and interstitial sites are replaced by cylinders and spheres, respectively.



Various lattices: **(a)** FCC, **(b)** BCC, and **(c)** A15 lattices.



(a) Rhombic dodecahedron – FCC lattice, **(b)** Kelvin's tetrakaidecahedron - BCC lattice and **(c)** Weaire-Phelan minimal surface - A15 lattice.



Structure of dendrimers that form the A15 lattice. A first generation dendrimer consists of a core segment and three dodecyl chains, a second generation dendrimer includes three first generation dendrimers attached to a core segment, and so on.

Supramolecular dendritic liquid quasicrystals

Nature 428, 157-159 (2004)

Xiangbing Zeng¹, Goran Ungar¹, Yongsong Liu¹, Virgil Percec²,
Andrés E. Dulcey² & Jamie K. Hobbs³

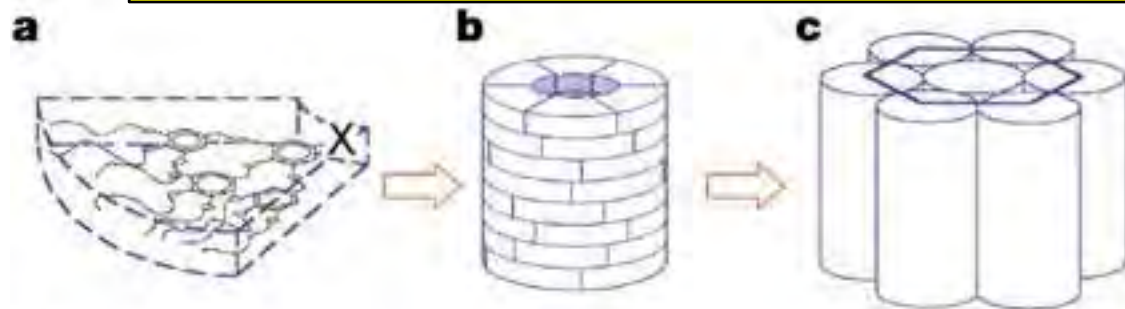
¹Department of Engineering Materials, University of Sheffield, Sheffield
S1 3JD, UK

²Roy & Diana Vagelos Laboratories, Department of Chemistry, University of

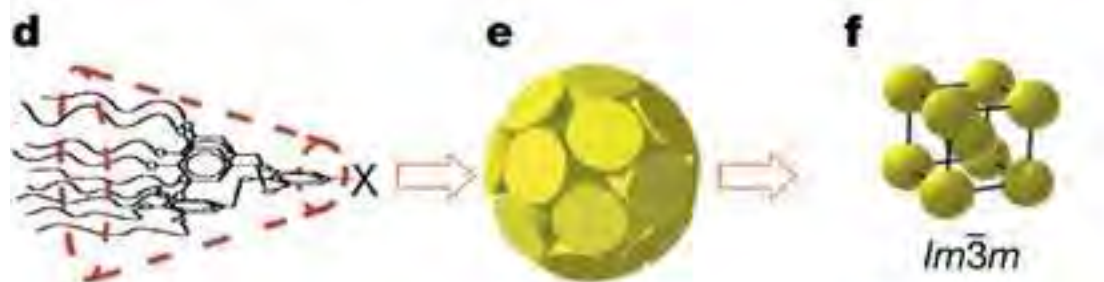


A large number of synthetic and natural compounds self-organize into bulk phases exhibiting periodicities on the 10-1000 nm due to their molecular shape, degree of amphiphilic character and, often, the presence of additional non-covalent interactions. Such phases are found in lyotropic systems (lipid–water, soap–water), in block copolymers and in thermotropic (solvent-free) liquid crystals. The resulting periodicity can be 1D (lamellar phases), 2D (columnar phases) or 3D (‘micellar’ or ‘bicontinuous’ phases). All such 2D and 3D structures identified to date obey rules of crystallography and their symmetry can be described, respectively, by one of the 17 plane groups or 230 space groups. **The ‘micellar’ phases have crystallographic counterparts in transition-metal alloys, with one metal atom is equivalent to a 1,000 – 10,000-atom micelle.** However, some metal alloys are known to defy the rules and form so-called quasicrystals, which have rotational symmetry other than the allowed 2-, 3-, 4- or 6-fold symmetry. **Here we show that such quasiperiodic structures can also exist in the scaled-up micellar phases, representing a new mode of organization in soft matter.**

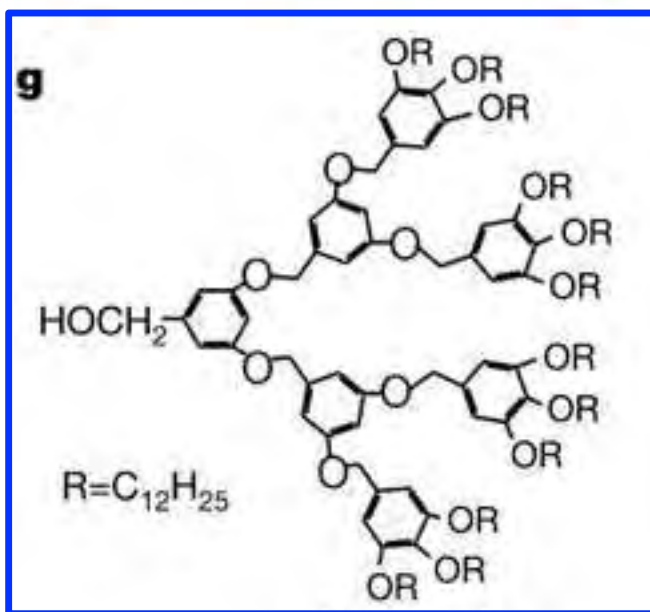
Self-assembly of wedge-shaped molecules



a) Dendrons with few tethered chains adopt a flat slice-like shape (X = weak binding group). **c)** The slices stack up and form cylindrical columns, which assemble on a 2D hexagonal columnar lattice.



d) Dendrons with more end-chains = conical shaped, which **e)** assemble into spheres that pack, **f)** on 3D lattices ($Im\bar{3}m$, $Pm\bar{3}n$, and $P4_2/mnm$).



Dendron I



g) Structure of Dendron I.

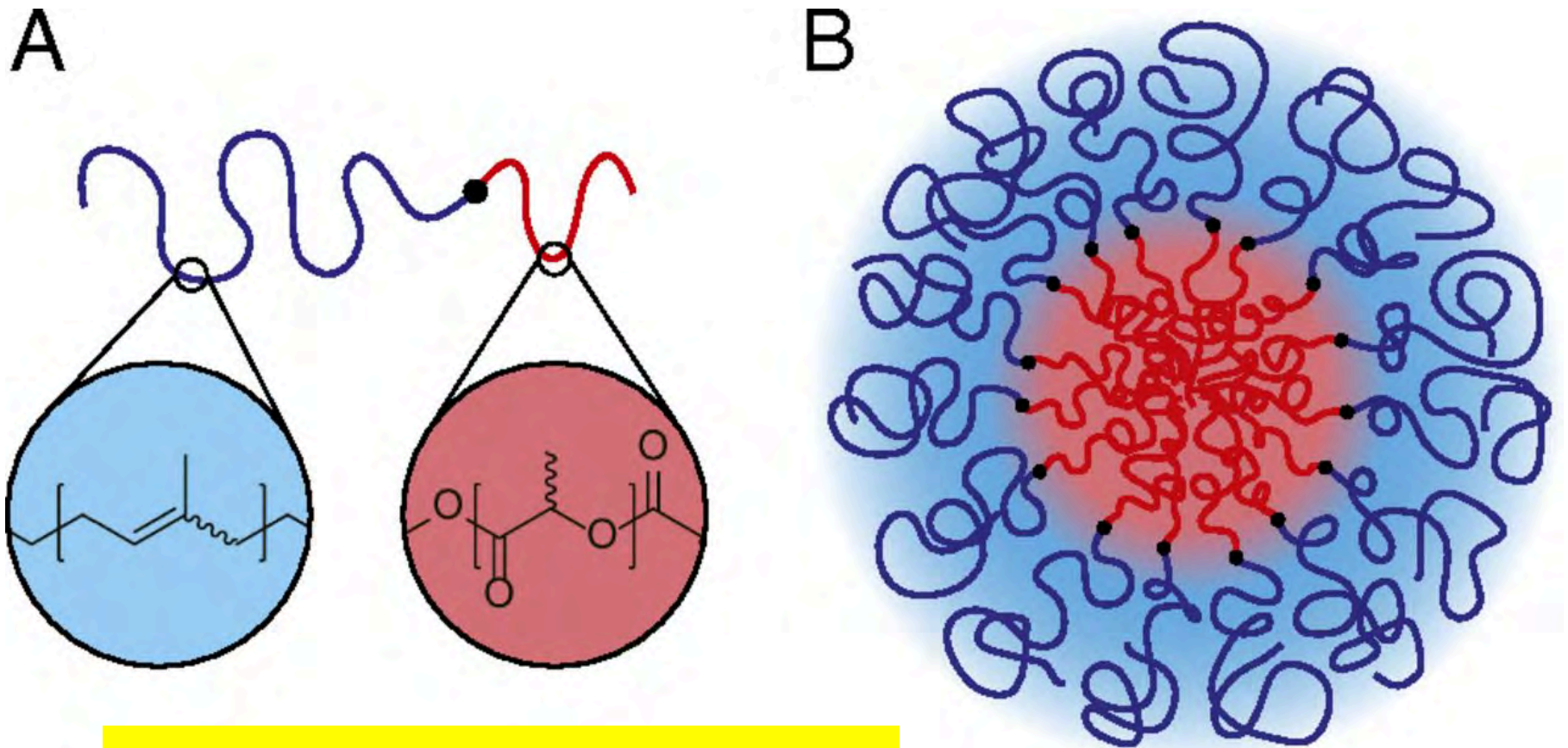
Discovery of a Frank-Kasper σ Phase in Sphere-Forming Block Copolymer Melts

Sangwoo Lee, Michael J. Bluemle,* Frank S. Bates† SCIENCE VOL 330 15 OCTOBER 2010

Sphere-forming block copolymers are known to self-assemble into BCC crystals near the order-disorder transition temperature. SAXS and TEM experiments on diblock and tetrablock copolymer melts have revealed an equilibrium phase characterized by a large tetragonal unit cell containing 30 microphase-separated spheres. This structure, referred to as the sigma (σ) phase by Frank & Kasper > 50 years ago, nucleates & grows from the BCC phase similar to its occurrence in metal alloys and is a crystal approximant to dodecagonal quasicrystals. Formation of the σ phase in undiluted linear block copolymers (& certain branched dendrimers) appears to be mediated by macromolecular packing frustration, an entropic contribution to the interparticle interactions that control the sphere-packing geometry.

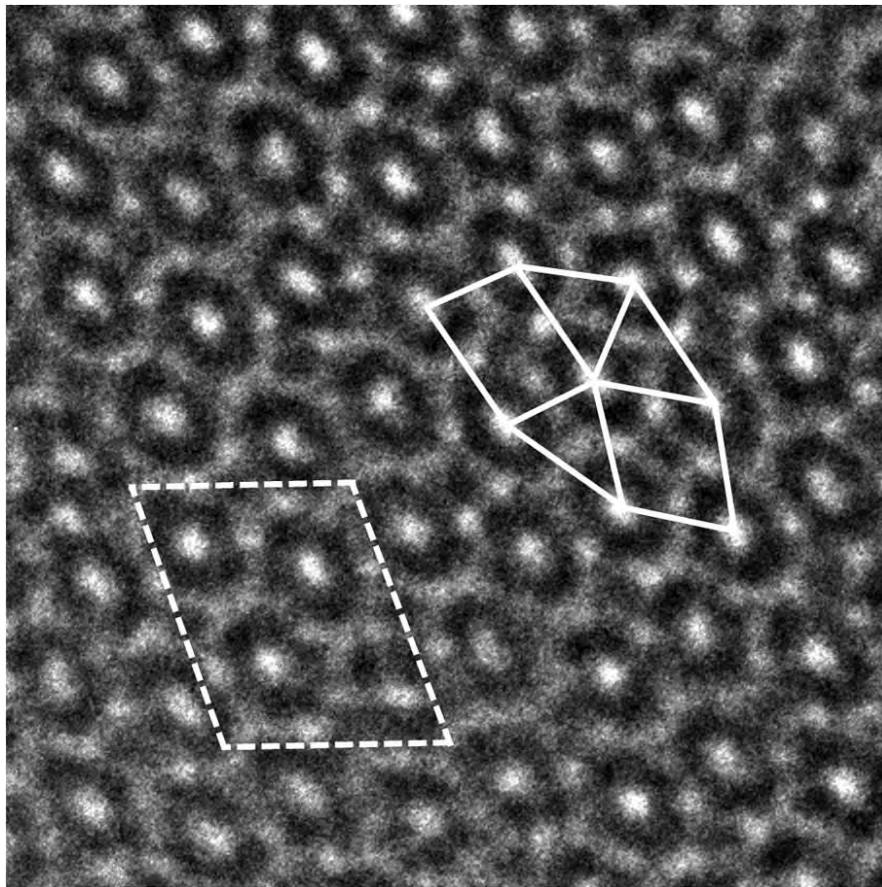


Schematic: (A) molecular structure of poly(isoprene-b-lactide) diblock copolymer, and (B) an isolated self-assembled spherical micelle.



Hydrophilic on inside, so reverse of micelle in aqueous solution

TEM image recorded from a stained thin section of SISO-3. The morphology is consistent with a tilted c-axis projection of the σ phase, where the unit cell is identified by the dashed rectangle. Isolated white spots surrounded by dark and gray rings are consistent with columns of dodecagonal units of spheres. A five-fold coordinated **3².4.3.4 tiling** element, formed from squares and triangles, is associated with each ring in the morphology, verifying the assignment of the σ phase.



50 nm

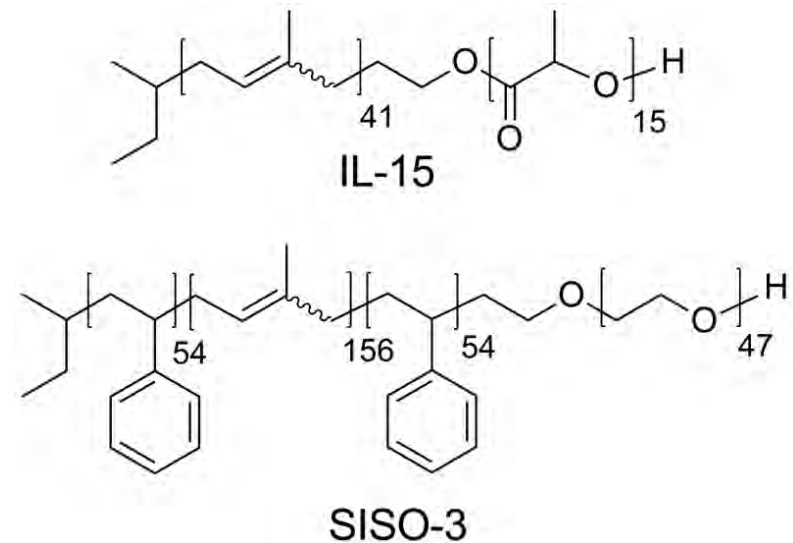
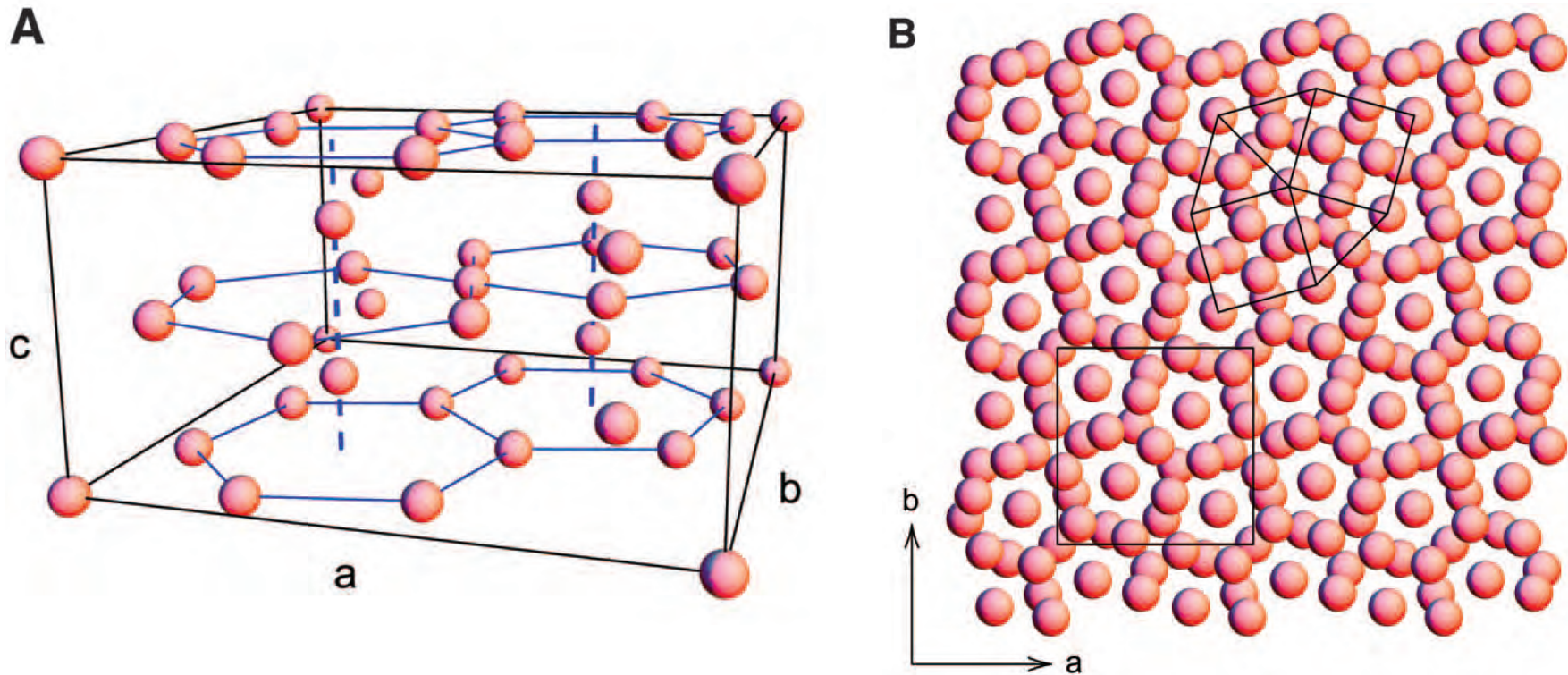


Fig. 1. Molecular architecture of poly(isoprene-*b*-lactide) (IL) and poly(styrene-*b*-isoprene-*b*-styrene-*b*-ethylene oxide) (SISO).

(A) Unit cell for the σ -phase morphology ($P4_2/mnm$ symmetry) based on a Rietveld analysis of the IL-15 SAXS powder pattern. Columns of spheres (dashed blue lines) surrounded by fused rings of hexagonally coordinated spheres (solid blue lines) produce a distinctive pattern when projected along the c axis (B), which is consistent with the TEM image. A $3^2.4.3.4$ tiling element, characteristic of the five-fold coordination of the dodecagonal elements in the σ phase, and the tetragonal face of the unit cell, are sketched on this image.



Sphericity and symmetry breaking in the formation of Frank–Kasper phases from one component materials

Sangwoo Lee^{a,b}, Chris Leighton^b, and Frank S. Bates^{b,1}

^aDepartment of Chemical and Biological Engineering, Rensselaer Polytechnic Institute, Troy, NY 12180; and ^bDepartment of Chemical Engineering and Materials Science, University of Minnesota, Minneapolis, MN 55455

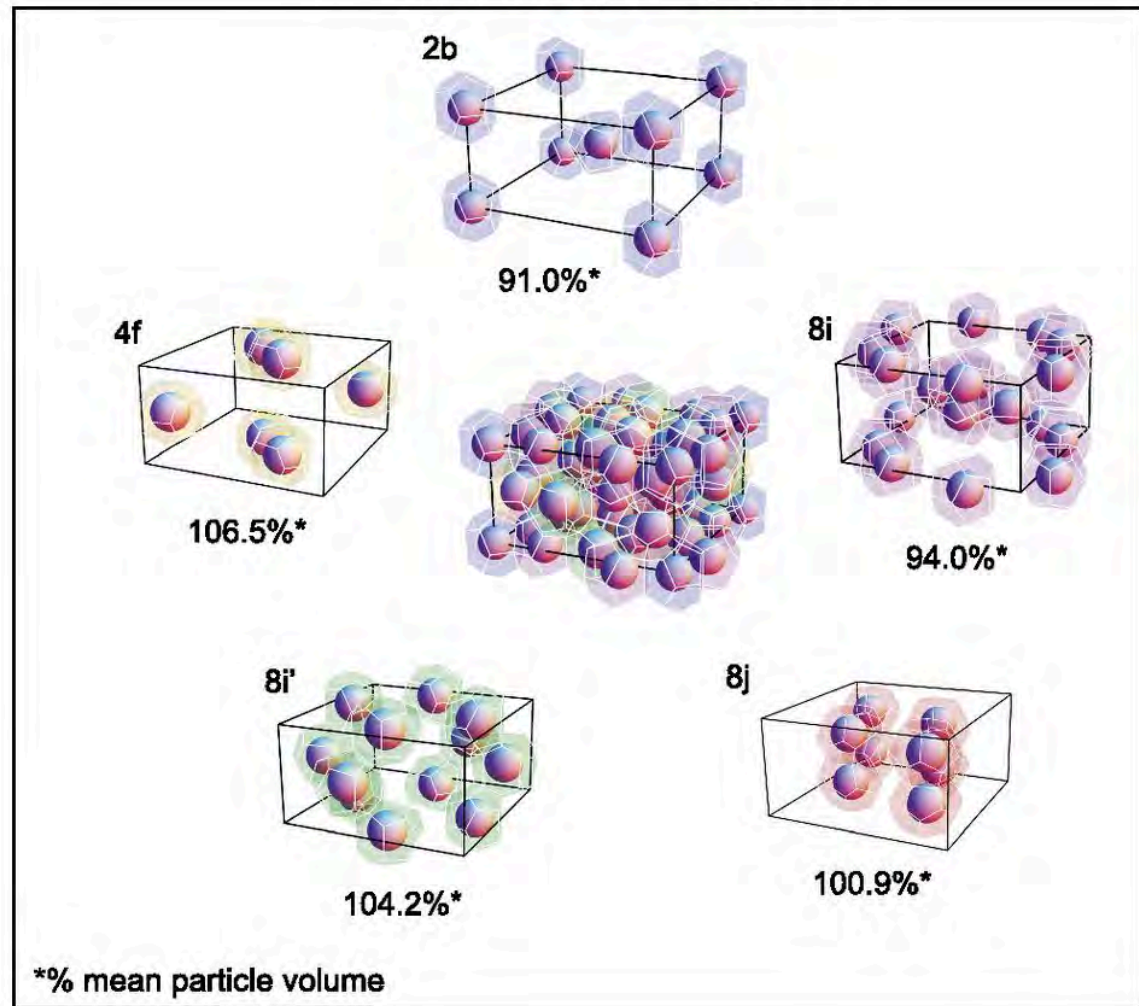
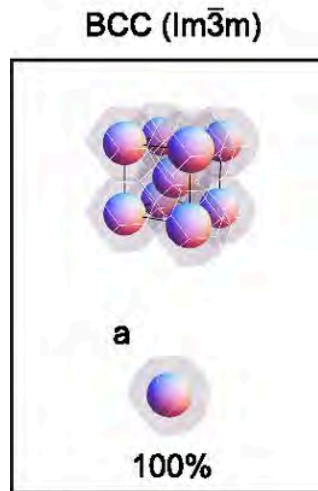
This Feature Article is part of a series identified by the Editorial Board as reporting findings of exceptional significance.

Edited by Salvatore Torquato, Princeton University, Princeton, NJ, and accepted by the Editorial Board October 1, 2014 (received for review May 13, 2014)

Understanding how particles fill space has challenged mathematicians, scientists, and technologists since antiquity. This article rationalizes the spontaneous organization of single-component diblock copolymers into multimolecular nanoscale domains that order into a low-symmetry Frank–Kasper (FK) phase with short-range tetrahedral close packing and a giant unit cell that contains 30 particles. This class of crystal structures bridges conventional periodic crystals and low symmetry aperiodic crystals often termed “quasicrystals.” Surprising analogies are thus drawn between the heretofore unexplained formation of FK structures in soft materials, and in certain elemental metals (including manganese and uranium), alloys, and intermetallic compounds, highlighting opportunities to better understand space filling in hard and soft materials by investigation of block polymers with precisely tuned molecular architectures.

PNAS 111 (50): 17723–17731 (2014)
doi: 10.1073/pnas.1408678111

Frank-Kasper σ -phase ($P4_2/mnm$)



Space-filling representations of BCC & Frank–Kasper σ phases. Faceted polyhedra represent self-assembled particles that must fill space at uniform density, with distortions in size & shape imposed by lattice symmetry. BCC has one particle / lattice site, with **~193 copolymers**. The σ -phase has 30 **particles** / lattice site, over 5 polyhedra with varying size & shape, at the indicated Wyckoff positions: 2b, 4f, 8i, 8i', 8j. **Different polyhedra-volumes demand varying numbers of molecules per particle between 176 (91%) and 206 (106.5%) !!**

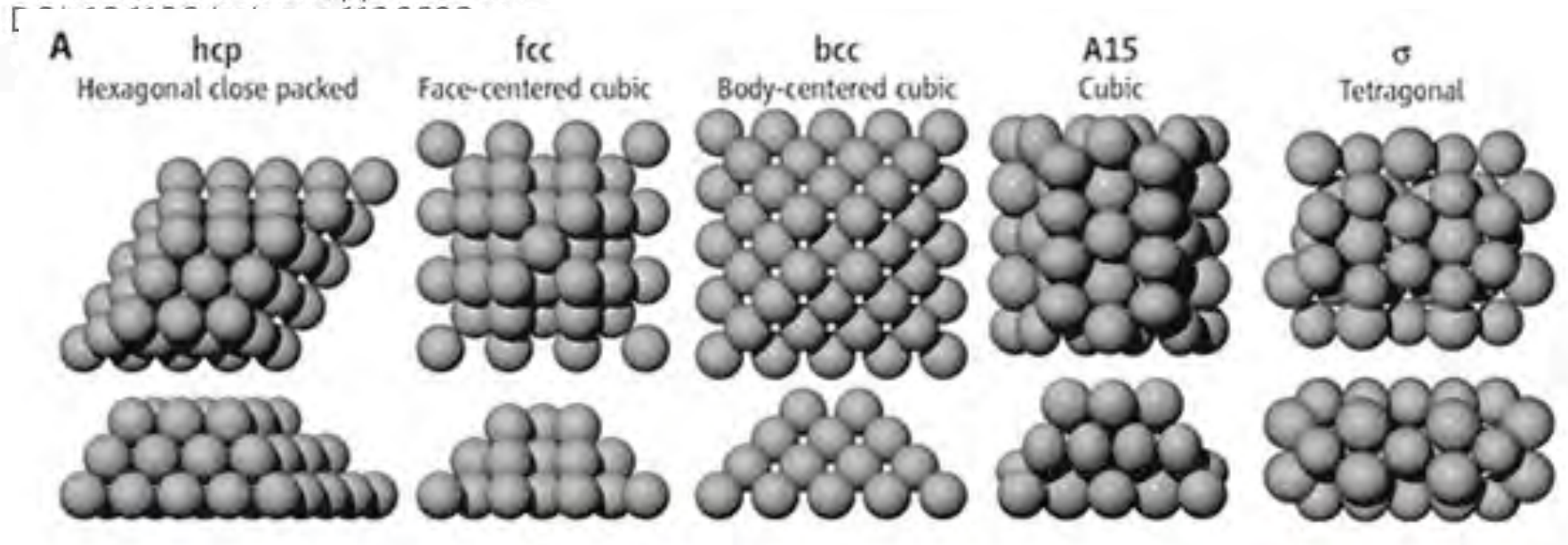
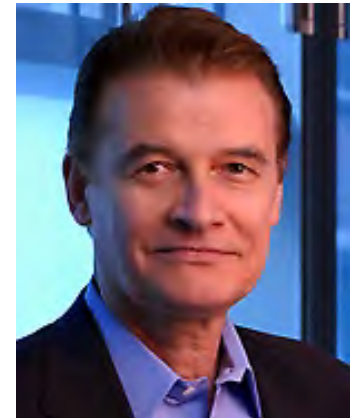
Recasting Metal Alloy Phases with Block Copolymers

Mihai Peterca and Virgil Percec*

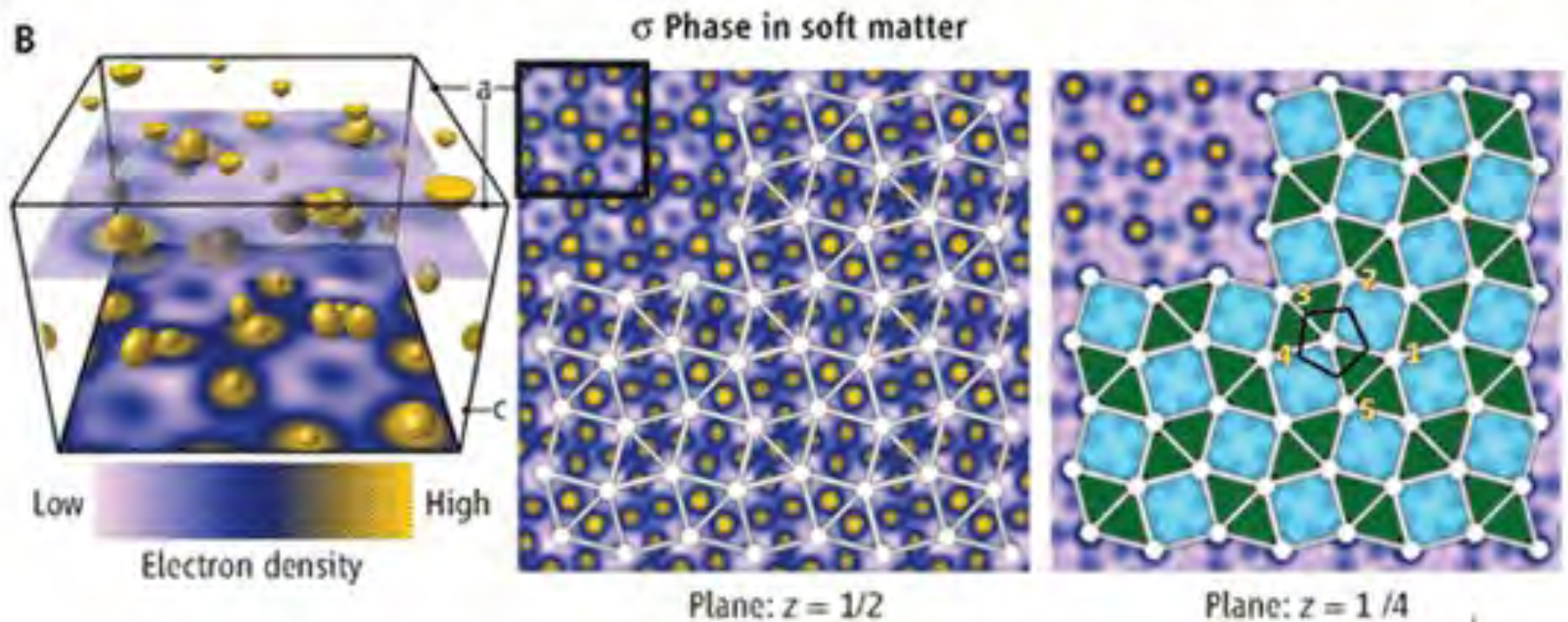
+ Author Affiliations

*To whom correspondence should be addressed. E-mail: percec@sas.upenn.edu

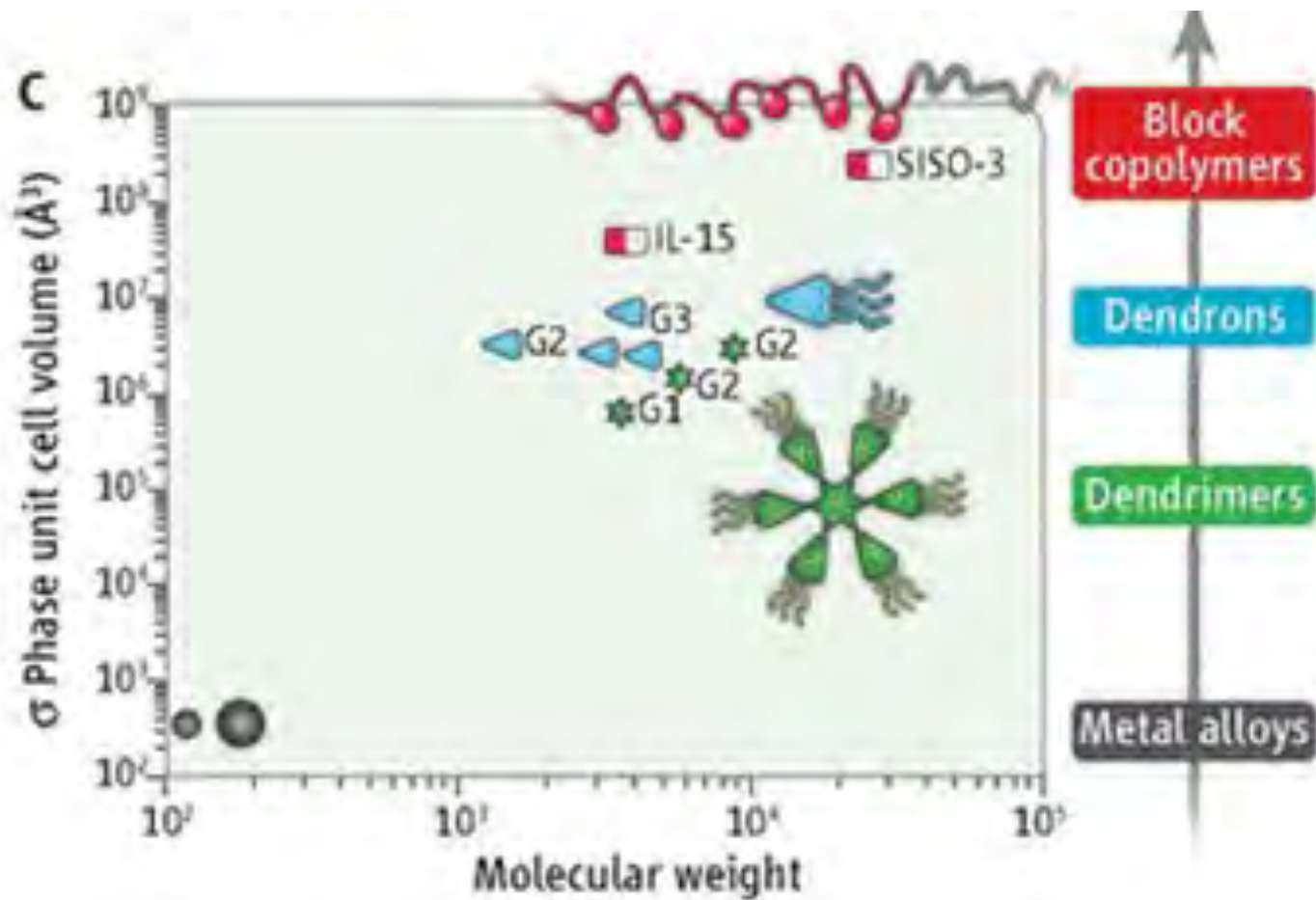
Science 15 Oct 2010;
Vol. 330, Issue 6002, pp. 333-334



A) Close-packed spheres can group together to fill space in different arrangements



(B) Electron density distribution of the σ phase formed from soft macromolecules. Overlaid squares and triangles mark the unusual periodic packing within the alternating layers (planes $z = 1/2$ and $z = 1/4$) formed by spherical assemblies with five nearest neighbors.



(C) Dependence of molecular weight of the building block and unit cell volume for the σ phase illustrating the scaling-up principle in soft matter. The large unit cells result from spherical aggregates formed by hundreds of individual polymers.



END

